RSC Advances

PAPER

View Article Online
View Journal | View Issue

Cite this: *RSC Adv.*, 2014, **4**, 13533

Synthesis and discovery of andrographolide derivatives as non-steroidal farnesoid X receptor (FXR) antagonists†

Zhuyun Liu,‡[a] Wai-Kit Law,[b] Decai Wang,[a] Xin Nie,[a] Dekuan Sheng,[a] Genrui Song,[a] Kai Guo,[c] Ping Wei,[c] Pingkai Ouyang,[c] Chi-Wai Wong*[b] and Guo-Chun Zhou*[a]

Received 15th November 2013
Accepted 28th January 2014

DOI: 10.1039/c3ra46715e

www.rsc.org/advances

Based upon the discovery of the natural compound andrographolide (**1**) as a non-steroidal farnesoid X receptor (FXR) antagonist, a series of andrographolide derivatives were designed and synthesized accordingly. Our primary SAR studies demonstrated that 14-phenoxy andrographolide scaffold is an excellent structural pharmacophore for FXR antagonists. Remarkably, 14β-compounds of **12b**, **12f** and **10g** were found to be the most potent FXR antagonists in this work. Structural docking discovered that the phenoxy substitution at the 14-position and the modification at 3,19-positions altered the putative binding positions of small FXR ligands, resulting in their FXR antagonistic activity discrepancy.

Introduction

Nuclear receptors are classified as ligand-activated transcription factors that regulate the expression of specific target genes and are involved in several physiological functions including reproduction, development, and metabolism.[1] Farnesoid X receptor (FXR), also known as bile acid receptor (BAR) or NR1H4, is a nuclear receptor that is encoded by the *NR1H4* gene in humans and expressed at high levels in the liver, intestine and other cholesterol-rich tissues.[1,2] Cholic acid (CA), chenodeoxycholic acid (CDCA), and other bile acids are natural ligands[2–5] for FXR (Fig. 1).

After activated by bile acid ligand/s,[2–5] FXR translocates to the cell nucleus, where FXR recruits retinoid X receptor (RXR) to form a heterodimer and then binds to hormone response elements on DNA, which up- or down-regulates the expression of certain genes.[1,2] The down-regulation of CYP7A1 (ref. 21) (cholesterol 7α-hydroxylase) of the rate-limiting enzyme in bile acid synthesis from cholesterol is one of the primary functions of FXR activation, resulting in a negative feedback in which synthesis of bile acids is inhibited if the cellular levels of bile acids are high.[1–5] It is reported that FXR has an active role in regulating cholesterol, lipoprotein, and glucose metabolism and its association with liver disease,[22,23] liver regeneration[24] and tumorigenesis,[25] suggesting that FXR represents an attractive pharmacological target.[26,27]

Currently, most studies are focused on FXR agonists (Fig. 1).[6–11] Because it is possible that FXR over-regulation causes some diseases and an unnatural FXR agonist diverts the normal pathway to result in potentially undesirable side effects,[25–28] it is necessary to develop FXR antagonists as FXR modulators.

The known FXR antagonists[12–20] (Fig. 1) are mainly derived from a steroidal scaffold and a finite number of other structural skeletons have been reported in recent years. Thus, seeking potent, structurally diverse and non-steroidal FXR antagonists should be an important step forward in this field. The utilization of natural products as a source of structural or functional diversity for the design and synthesis of novel molecules has been an important aspect of new drug design.[29,30] So as to increase structural diversity of FXR antagonists, we launched a project initiated by the high-throughput screening of the natural compound libraries from a series of Traditional Chinese Medicines (TCMs) based on FXR luciferase activity assay.[31] Andrographolide (**1**, Fig. 1),[32,33] a diterpene ester from *Andrographis panniculata* (Burm.f.) Nees, was identified as a weak FXR antagonist (IC_{50} = 9.7 μM, Fig. 2).

Andrographolide (**1**) is the representative active ingredient of *Andrographis panniculata* (Burm.f.) Nees and it works as a broad therapeutic agent.[34,35] Although **1** has a molecular weight of 350 Da, 3 hydrogen bond donors, 5 hydrogen bond acceptors and 2.1186 of the calculated Log *P* (Table S1†, entry 23), which conforms to the "Rule of Five", its poor water-solubility and also relatively low lipo-solubility, weak potency

[a]*School of Pharmaceutical Sciences, Nanjing Tech University, Nanjing 211816, P. R. China. E-mail: gczhou@njtech.edu.cn; Tel: +86-25-58139415*

[b]*NeuMed Pharmaceuticals Limited, Shatin, N. T., Hong Kong, P. R. China. E-mail: wongcw@neumedpharma.com.hk; Tel: +852-67487218*

[c]*College of Biotechnology and Pharmaceutical Engineering, Nanjing Tech University, Nanjing 211816, P. R. China*

† Electronic supplementary information (ESI) available: Table S1, ^{1}H NMR and ^{13}C NMR spectra of compounds **5–13**. CCDC 960845. For ESI and crystallographic data in CIF or other electronic format see DOI: 10.1039/c3ra46715e

‡ Current address: Department of Pharmaceutical and Chemical Engineering, Taizhou Polytechnic College, Taizhou 225300, Jiangsu, PR China.

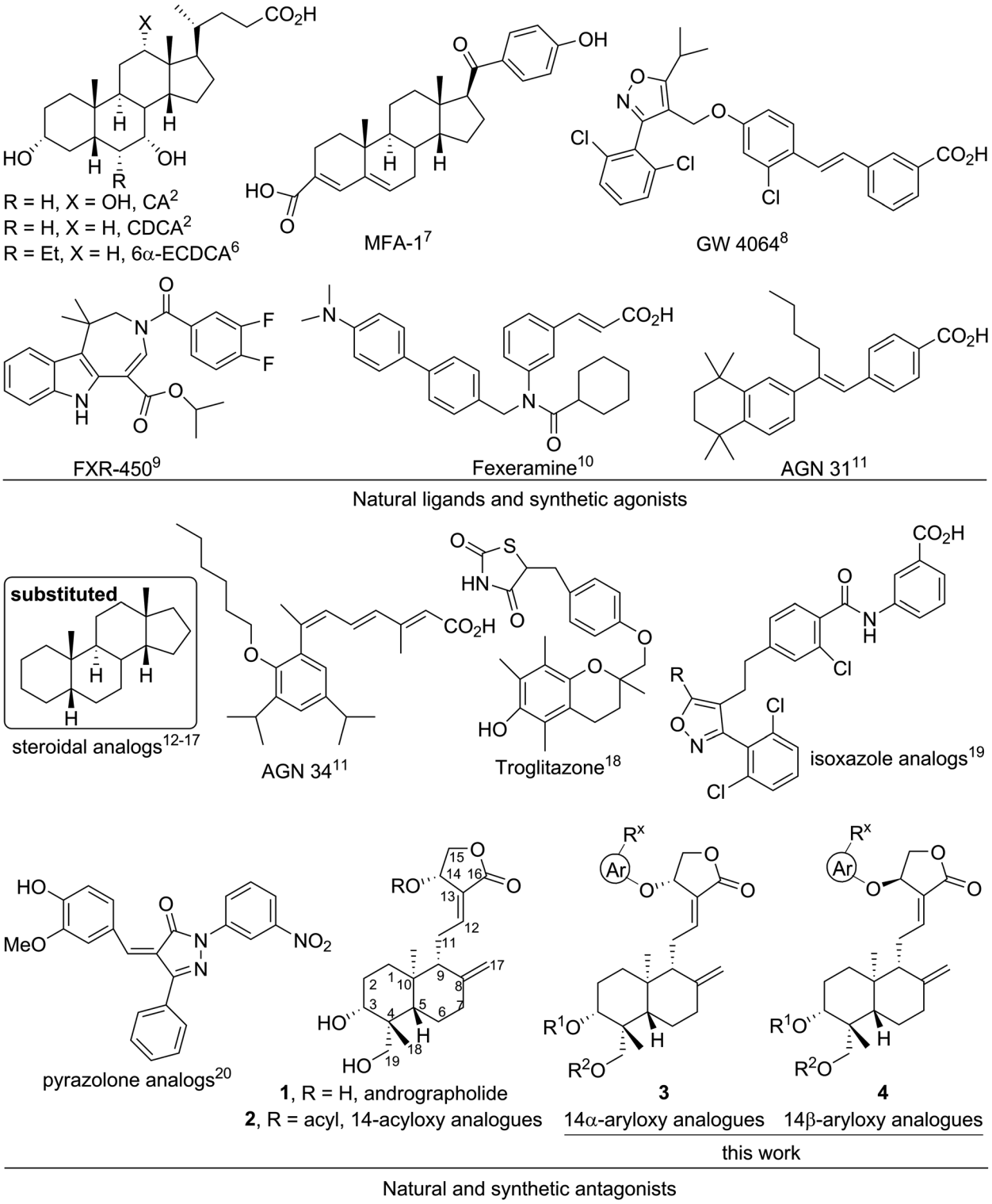

Fig. 1 Natural and synthetic known ligands for FXR and general structures of andrographolide and their derivatives.

and inadequate therapeutic efficacy restrict its further application. To improve its physiochemical properties and pharmaceutical features, numerous andrographolide derivatives have been reported from time to time, especially preparation of 14-acyloxy andrographolide derivatives[36–40] (**2**, Fig. 1). Herein, we describe the synthesis and SAR studies of 14-aryloxy andrographolide derivatives (**3** and **4**, Fig. 1), leading to the identification of a series of 14-phenoxy andrographolide derivatives as more potent FXR antagonists than the lead andrographolide (**1**).[41]

Results and discussion

In our preliminary study, andrographolide (**1**) was found to be a weak FXR antagonist (IC_{50} = 9.7 μM) in the concentration-dependent mode (Fig. 2),[31] this result spurred us on to discover more potent FXR antagonists on the basis of andrographolide derivatives. As 14-acyloxy andrographolide esters (**2**, Fig. 1) were effective in some reported studies for other assays,[36–38] we were interested in investigating 14-modified andrographolide derivatives as FXR novel antagonists.

In an initial exploration step, some simple derivatives of andrographolide were studied (Scheme 1). Starting from **1**, 3,19-acetonylidene protection was conducted in DCM and catalyzed by PPTS yielding **5** as reported.[36–38] Inversion of 14α-OH of **5** into 14β-OAc of **6** was achieved by Mitsunobu reaction under normal conditions. 14-Epimeric andrographolide (**8**) or its 14β-acetylated derivative (**7**) was generated in MeOH/H_2O (4/1) with TsOH·H_2O by partial (at 20 °C) or complete (40 °C) hydrolysis of **6**, respectively. Finally, 14β-3,19-acetonylidene derivative (**9**) was made by the same preparation conditions as **5**.

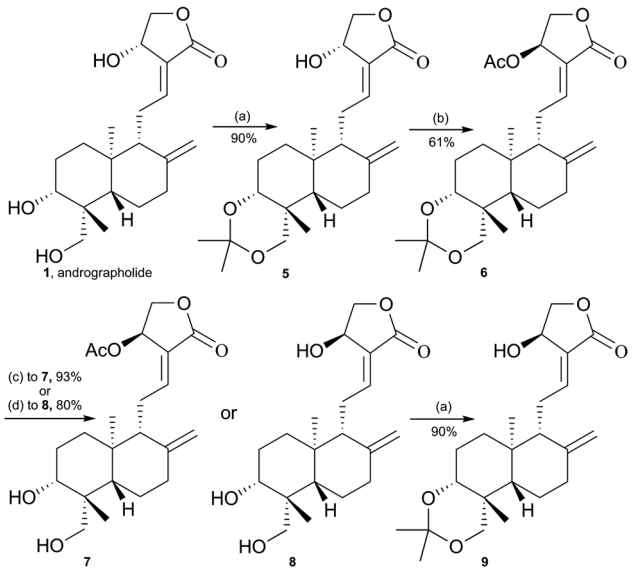

Scheme 1 Reagents and conditions: (a) anhydrous DCM, 2,2-dimethoxypropane, PPTS, 40 °C; (b) anhydrous THF; **5** (1.0 eq.), anhydrous HOAc (1.5 eq.), DIAD (1.5 eq.), PPh_3 (1.5 eq.), 0 °C to room temperature; (c) MeOH/H_2O (4/1), TsOH·H_2O, 20 °C; (d) MeOH/H_2O (4/1), TsOH·H_2O, 40 °C.

FXR antagonistic results of the synthesized compounds were measured by the luciferase reporter assay[31] and shown in Table 1 (entries 23–28). The antagonistic potencies at 5.0 μM are depicted in Fig. 2. Compared to **1**, 3,19-isopropylidene andrographolide (**5**) slightly improved the FXR antagonistic activity. 14β-Epimeric andrographolide (**8**) was a much weaker FXR antagonist than **1** and 14β-acetylated andrographolide (**7**) became inactive to FXR. Unlike the relationship between **1** and **5**, 3,19-isopropylidene 14β-andrographolide (**9**) was indeed a weaker FXR antagonist than **8**. 14β-Acetylated 3,19-isopropylidene andrographolide (**6**) is more active than 14β-acetylated 3,9-diol analogue **7** in antagonizing FXR. By comparison of 14β-andrographolide (**8**) with its modified derivatives (**6**, **7**, **9**), it was discovered that 3,19-isopropylidene modification alone (**9**) almost did not change the antagonistic activity and 14-acetylation modification alone (**7**) decreased the antagonistic activity, but simultaneous modifications (**6**) of 3,19-isopropylidene and 14-acetylation enhanced somewhat the antagonistic activity. It was inferred from these preliminary data (Fig. 2 and Table 1, entries 23–28) that the optimal combination of 3,19- and 14-modifications including 14α- or 14β-configuration is possibly helpful for the FXR antagonistic activity.

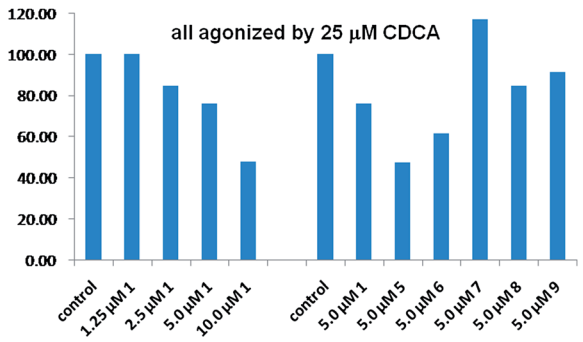

Fig. 2 The FXR antagonistic activities of compounds **1** and **5**–**9**. Control (100%) is the activity of FXR in the presence of 25.0 μM CDCA.

Considering that aryloxy ether is chemically more stable than the acyloxy ester, we are interested in 14-aryloxy ether analogues of andrographolide (Fig. 1) in our exploration. Incrementing the structural diversity is the important superiority of 14-aryloxy ether by the utilizing of varied aromatic skeletons (*e.g.* phenyl, naphthyl, quinolinyl, pyridinyl, *etc.*) and the incorporation of different substituents into aromatic scaffolds. In this work, 14-phenoxy andrographolide derivatives (Ar = Ph, Fig. 1, series **3** and **4**) were firstly studied.

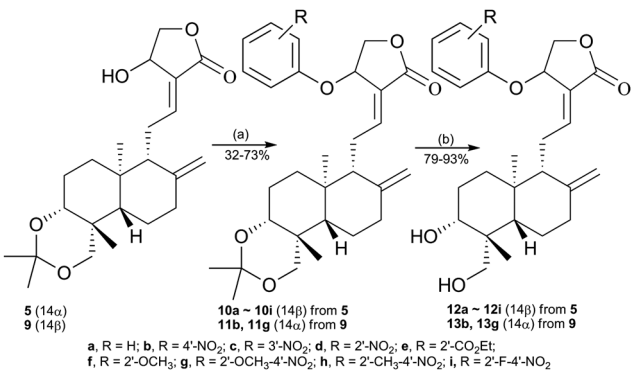

Scheme 2 Reagents and conditions: (a) anhydrous THF; **5** or **9** (1.0 eq.), phenol (1.5 eq.), DIAD (1.5 eq.), PPh_3 (1.5 eq.), 0 °C to room temperature; (b) MeOH/H_2O (4/1), TsOH·H_2O, 20 °C.

As shown in Scheme 2, 14α-compound **5** or its 14β-epimer **9** were used as starting materials for the synthesis of 14β- or 14α-phenoxy andrographolide derivatives, respectively. The key

synthetic approach to 14-phenoxy andrographolide derivatives is the Mitsunobu reaction. Diverse phenols were used to prepare two series of 14β-phenoxy (**10**) and 14α-phenoxy (**11**) compounds. The reaction was performed in general from 0 °C to room temperature in anhydrous THF and afforded **10** or **11** in mild to moderate isolated yield depending on the distinct phenol property. Removal of the protective group of 3,19-acetonylidene from **10** or **11** by $TsOH \cdot H_2O$ in $MeOH/H_2O$ (4/1) at 20 °C, the series of compounds **12** or **13** were obtained in high yields, respectively. It is worthwhile noting that α-isomers of **11** and **13** were generally less stable than their corresponding β-isomers of **10** and **12**.

In order to confirm the stereochemistry of C-14 in these series, the single crystal of **10b** was cropped from petroleum ether/ethyl acetate (5/4) and its crystal structure was determined as shown in Fig. 3a by X-ray crystallography, which is in accordance with our expected structure. The crystal packing diagram (Fig. 3b) of **10b** demonstrated that the molecule **10b** is stabilized and linked by the intermolecular hydrogen bonds of C(9)–H(β)···O(4′-NO_2) and C(14)–H(α)···O(lactone)–C(15).

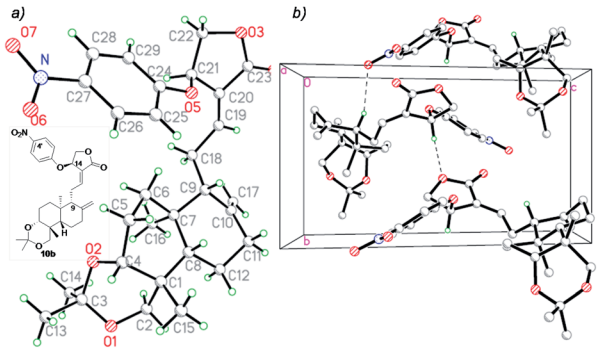

Fig. 3 Molecular and crystal structures (a) and crystal packing diagram (b) of **10b**. ESI.†

The calculated data of "Lipinski's Rule of Five" of **1** and these synthesized compounds **5–9** and **10–13** are included in Table S1.† Even some of these compounds do not conform very well to the "Rule of Five"; they have the potential to be optimized and developed into drug-like candidates in the future. FXR antagonistic activity and the cellular toxicity of **1** and these synthesized compounds **5–9**, and **10–13** are listed in Table 1.

At first, 14β-phenoxy andrographolide derivative **10a** bearing the 3,19-acetonylidene group was found to be inactive (Table 1, entry 1); however, its hydrolyzed product of 3,19-diol **12a** (Table 1, entry 2) exhibited as a moderate FXR antagonist (IC_{50} = 5.7 μM), is better than our lead **1**. Then, we moved to incorporate substituted groups into the phenyl ring at the 14-position to investigate the structure–activity relationship (SAR). 4′-Nitrophenoxy compounds of **10b** with 3,19-acetonylidene group and **12b** of 3,19-diol derivative were designed and tested. Compound **10b** (IC_{50} = 8.6 μM; Table 1, entry 3) is less potent than **12a** but it is much more active than its corresponding counterpart **10a** as a FXR antagonist; notably, the IC_{50} value of **12b** reached 0.55 μM (Table 1, entry 4) in the FXR antagonistic activity, indicating that the 14-(4′-nitrophenoxy) group is an important pharmacophore (**10a** < **10b** and **12a** < **12b**). In addition, it seems that the 3,19-acetonylidene group decreases the FXR antagonistic activity (**10a** < **12a** and **10b** < **12b**) for these compounds.

Table 1 FXR antagonistic activity of synthesized compounds **1**, **5–9**, **10–13**

Entry	Cmpd[a]	R	14-Isomer	IC_{50}[b]	CC_{50}[c]
1	**10a**	H	β	NA	—
2	**12a**	H	β	5.7	>15.0
3	**10b**	4′-NO_2	β	8.6	>15.0
4	**12b**	4′-NO_2	β	0.55	>15.0
5	**10c**	3′-NO_2	β	NA	—
6	**12c**	3′-NO_2	β	NA	—
7	**10d**	2′-NO_2	β	3.0	8.5
8	**12d**	2′-NO_2	β	NA	—
9	**10e**	2′-CO_2Et	β	2.9	12.3
10	**12e**	2′-CO_2Et	β	3.5	>15.0
11	**10f**	2′-OCH_3	β	2.4	>15.0
12	**12f**	2′-OCH_3	β	0.98	>15.0
13	**10g**	2′-OCH_3-4′-NO_2	β	2.0	>15.0
14	**12g**	2′-OCH_3-4′-NO_2	β	11.9	>15.0
15	**10h**	2′-CH_3-4′-NO_2	β	6.3	>15.0
16	**12h**	2′-CH_3-4′-NO_2	β	NA	—
17	**10i**	2′-F-4′-NO_2	β	3.9	>15.0
18	**12i**	2′-F-4′-NO_2	β	NA	—
19	**11b**	4′-NO_2	α	15.1	>15.0
20	**13b**	4′-NO_2	α	16.0	>15.0
21	**11g**	2′-OCH_3-4′-NO_2	α	2.5	12.0
22	**13g**	2′-OCH_3-4′-NO_2	α	7.1	>15.0
23	**1**, Andrographolide		α	9.7	>15.0
24	**5**		α	9.0	>15.0
25	**6**		β	9.3	>15.0
26	**7**		β	NA	—
27	**8**		β	>15.0	—
28	**9**		β	>15.0	—

[a] See Scheme 2. [b] FXR-transfected 293T cells were agonized by 25.0 μM CDCA in all experiments and the vehicle control was set as 100%, "NA" means "not active". [c] The 293T cells were used to test compound's cellular toxicity, "—" represents "not detected".

After the above, 3′- and 2′-nitrophenoxy andrographolide derivatives **10c** and **12c**, **10d** and **12d**, respectively, were designed to investigate the effects of different nitro positions on the FXR antagonistic activity in comparison to 4′-nitrophenoxy analogues **10b** and **12b**. Among these, **10c** and **12c** of 3′-nitrophenoxy analogues, and **12d** of the 2′-nitrophenoxy analogue did not express FXR antagonistic activity (Table 1, entries 5, 6 and 8); nevertheless, **10d** of the 2′-nitrophenoxy analogue with 3,19-acetonylidene (Table 1, entry 7) showed a good FXR antagonistic activity (IC_{50} = 3.0 μM) but it possessed an obvious cellular toxicity (CC_{50} = 8.5 μM). Based upon these results, we further explored other substitution at the 2′-position of the 14-phenoxy group. Compound **10e** with an electron-withdrawing group of 2′-carboxylic ester (Table 1, entry 9) exhibited similar FXR antagonistic activity (IC_{50} = 2.9 μM) and cellular toxicity (CC_{50} = 12.3 μM) to its 2′-nitro counterpart **10d**. 2′-Carboxylic ester 3,19-diol compound **12e** (Table 1, entry 10), which is different from its inactive 2′-nitro-3,19-diol counterpart

12d, acted as a good FXR antagonist (IC_{50} = 3.5 μM) but did not show any obvious cellular toxicity. Interestingly, an electron-donating group of 2′-methoxy-substituted compound **10f** with 3,19-acetonylidene exhibited similar FXR antagonistic activity (IC_{50} = 2.4 μM, Table 1, entry 11) to **10d** and **10e** containing 2′-electron-withdrawing substitutions. Moreover, 2′-methoxy-3,19-diol **12f** was very active (IC_{50} = 0.98 μM, Table 1, entry 12) and its relatively low cellular toxicity was detected. Summarized from the above-mentioned results, it is concluded that the mono substitution at 2′-position is very flexible to the electron-donating group and the electron-withdrawing group for the FXR antagonistic activity, especially for **10** series compounds with the 3,19-acetonylidene group.

Inspired by these promising results of **12b** and **12f** bearing 4′-nitro and 2′-methoxy groups at 14-phenoxy, respectively, 2′-methoxy-4′-nitro-andrographolide derivatives **10g** and **12g** were logically designed (Fig. 4) and tested for their FXR antagonistic activity (Table 1 and Fig. 4). We envisioned that the "integration" of 2′-methoxy and 4′-nitro groups should retain or increase the antagonistic activity. Compared to its mother analogues **10b** (4′-nitro) and **10f** (2′-methoxy) with single substitution at 14-phenoxy, the dual substituted 2′-OMe-4′-NO_2 derivative **10g** with 3,19-acetonylidene (IC_{50} = 2.0 μM, Fig. 4 and Table 1, entry 13) was a more potent FXR antagonist than **10b** (IC_{50} = 8.6 μM) and **10f** (IC_{50} = 2.4 μM) as expected. However, it was surprising that 3,19-diol **12g** (IC_{50} = 11.9 μM) with dual substitutions at 14-phenoxy by 2′-methoxy group and 4′-nitro group (Fig. 4 and Table 1, entry 14) showed a much weaker FXR antagonistic activity than **10g** and its corresponding mother 3,19-diol analogues **12b** and **12f**, suggesting that the "integration" of 2′-methoxy and 4′-nitro groups affects the binding ability of these small molecules to FXR. More importantly, these data reveal that there are synergistic effects between substitutions at 14-phenoxy and 3,19-modifications on the antagonistic activities to the receptor FXR.

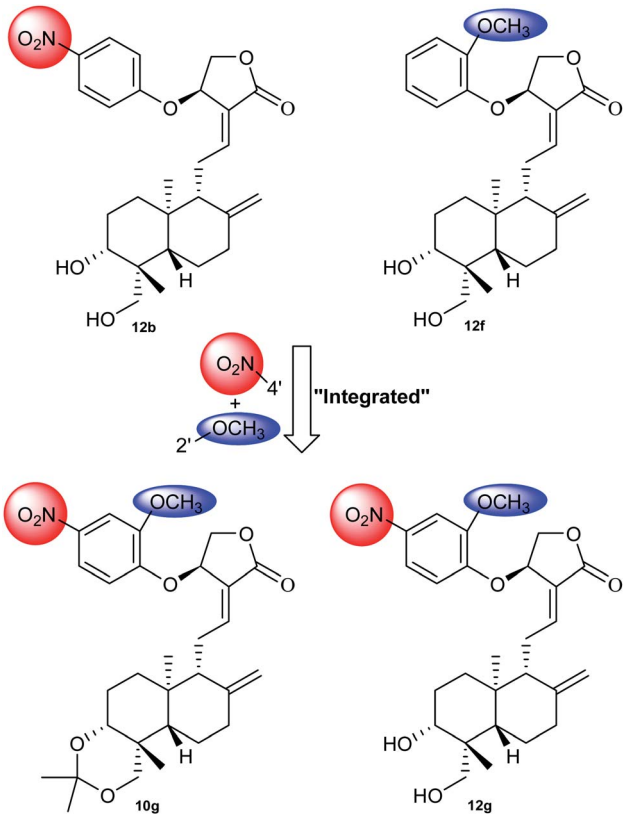

Fig. 4 Design of **10g** and **12g** from **12b** and **12f**.

As part of exploring the effects of 14-phenoxy substitutions on the FXR antagonistic activity, substituents of the methyl group as a weak electron-donating group and fluoro group as an electron-withdrawing group were introduced at the 2′-position into the 14-(4′-nitro)-phenoxy group, respectively. The assay data disclosed that 2′-methyl-4′-nitro derivative **10h** was a moderate FXR antagonist (IC_{50} = 6.3 μM, Table 1, entry 15) and its diol derivative **12h** lost its FXR antagonistic activity (Table 1, entry 16); meanwhile, introduction of 2′-fluoro at 14-(4′-nitro)-phenoxy made **10i** bearing 3,19-acetonylidene (IC_{50} = 3.9 μM, Table 1, entry 17) slightly more active than its 2′-methyl counterpart **10h** but its diol analogues **12i** (Table 1, entry 18) had a lack of FXR antagonistic activity as the 2′-methyl counterpart diol **12h**.

Taking into consideration that **1** is a 14α-isomer, we subsequently investigated 14α-(4′-nitro-phenoxy) and 14α-(2′-methoxy-4′-nitro-phenoxy) andrographolide analogues (Scheme 2 and Table 1, entries 19–22) since their corresponding 14β-isomers **12b** and **12g** are very potent FXR antagonists. Contrary to their 14β-isomers of **10b** and **12b**, two 14α-(4′-nitro)-phenoxy analogues of **11b** (IC_{50} = 15.1 μM, Table 1, entry 19) and **13b** (IC_{50} = 16.0 μM, Table 1, entry 20) were unfortunately weaker FXR antagonists than **1** (IC_{50} = 9.7 μM). **11g** (IC_{50} = 2.5 μM, Table 1, entry 21) of 3,19-acetonylidene-14α-(2′-methoxy-4′-nitro)-phenoxy derivative showed a similar FXR antagonistic activity to its 14β-counterpart **10g** (IC_{50} = 2.0 μM) but **11g** exhibited a cellular toxicity (CC_{50} = 12.0 μM); meanwhile, its corresponding diol **13g** (IC_{50} = 7.1 μM, Table 1, entry 22) was a moderate FXR antagonist. Thus, these data together with their decreased stability suggest that at the current stage, 14α-isomer analogues should not be considered further as FXR antagonists.

To decipher the structural basis for the above SARs, we compared the putative binding positions of compounds **1**, **5**, **6**, **10b**, **12b**, **10g** and **12g** by means of molecular docking. The docking model was generated from the chain A of 3DCT[42] from the same view using Discovery Studio 3.5 and the modelling results are shown in Fig. 5 and 6.

As shown in Fig. 5, even FXR antagonistic activities of **1**, **5** and **6** are similar, the putative binding positions of **1** (Fig. 5a), **5** (Fig. 5b) and **6** (Fig. 5c) in NS3 appear to be quite different, in which their orientation of decalin rings are distinctive, the bindings of lactone rings in **1** and **5** are similar but different from that in **6**. The putative binding position of **1** can be transformed into **5**'s by making a rotation of 180° along the bond of C9–C11 or C11–C12 or **6**'s by a rotation of 90° clockwise and then 180° along the bond of C9–C11 or C11–C12. These simulation results suggest that the spatial volume of the binding pocket in NS3 is large enough for different occupation modes which are dependent on the interaction between a specific ligand with the binding site. This means that optimal structural tuning will benefit binding potency.

Further, the predictive binding of the most potent compound of 3,19-diol **12b** is in good agreement with the large spatial

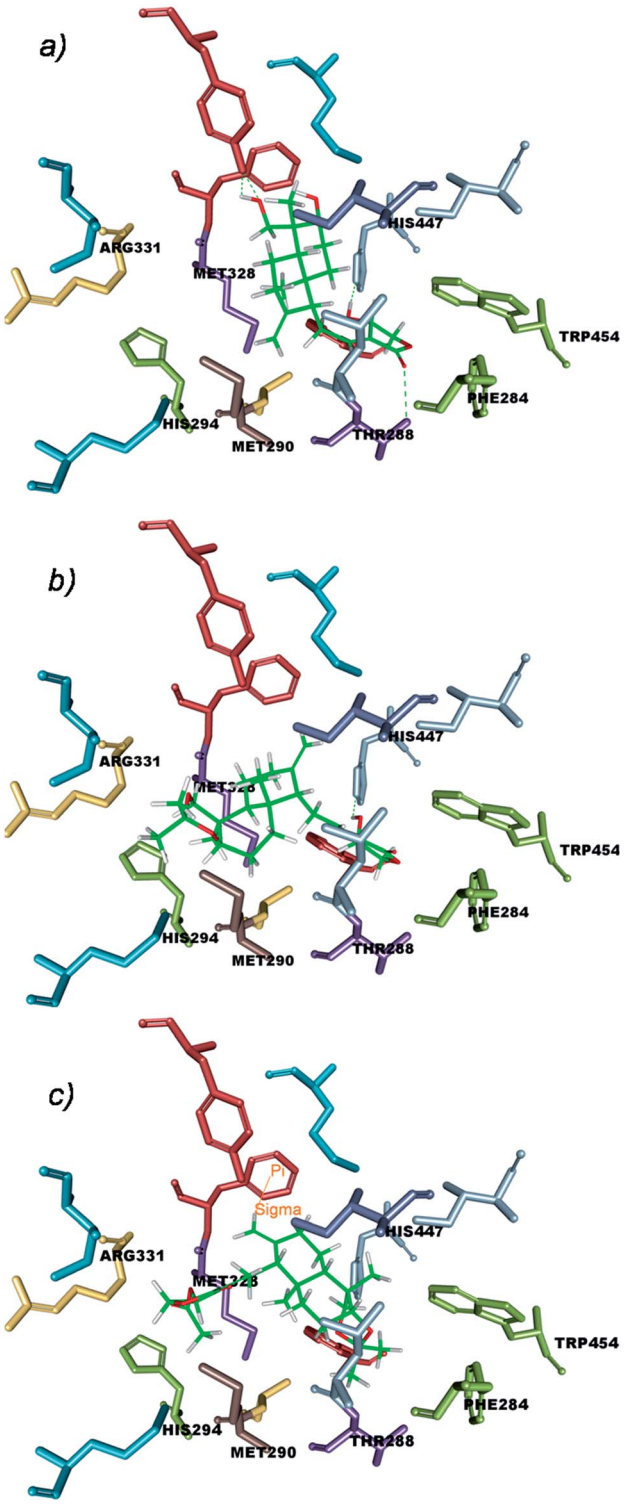

Fig. 5 Three-dimensional (3D) interaction diagrams of predicted binding positions of **1** (a), **5** (b) and **6** (c) in FXR active sites. Critical amino acid residues of the binding pocket are labelled. The green dash line denotes hydrogen bond between ligand and amino acid residue atoms of FXR protein.

volume binding pocket (Fig. 6b), in which there are two hydrogen bonds between the 4′-nitro group and the hydroxyl group of the Thr 288 residue and three π–π interactions of the 4′-nitro group with aromatic rings of Trp454 and Phe284, leading to the tight binding between **12b** and FXR (Fig. 6b). However, due to the relatively large and rigid 6-membered ring formed by 3,19-acetonylidene protection as indicated in Fig. 6a, compound **10b**, whose binding position is close to **5** but not **1** or **6**, was obstructed by the putative "gate" established by 4 amino acid residues of Met290, His294, Met328 and Arg331, which lets compound **10b** not fully enter the binding pocket, resulting in the loss of hydrogen bond and π–π interaction in the binding of **10b** to FXR. These molecular binding positions of **10b** and **12b** are in good agreement with their FXR antagonistic activities (**10b** < **12b**). Moreover, by comparison with the predictive binding positions of **10b** and **12b**, the orientations of 14β-(4′-nitro)-phenoxy moiety and the lactone ring of **10b** are reciprocally exchanged, suggesting the importance of their orientations for binding.

Since compounds **10g** and **12g** expressed big differences in their FXR antagonistic activities (**10g** > **12g**) and their SAR is totally distinct from that of **10b** and **12b** (**10b** < **12b**), we were interested in understanding how 2′-methoxy group affects the binding positions of **10g** and **12g**. Interestingly and notably, the predictive binding position of **10g** (Fig. 6c) bearing 3,19-acetonylidene protective group is different from that of its corresponding counterpart **10b** (Fig. 6a) but is quite similar to that of the diol **12b** (Fig. 6b); meanwhile, the predictive binding position of the diol **12g** (Fig. 6d) is not similar to that of the diol **12b** (Fig. 6b) but is almost identical to that of 3,19-acetonylidene protected compound **10b** (Fig. 6a), these observations gave a good explanation for the above-mentioned FXR antagonistic relationship of **10b** < **12b** *vs.* **10g** > **12g** (Fig. 6 and Table 1, entries 1, 2, 13 and 14). Except for one more hydrogen bond in the binding pose of **12b** as shown in Fig. 6b, the interaction of **10g** with FXR (Fig. 6c), which is stabilized by one hydrogen bond and three π–π interactions, is similar to **12b**. Because 3,19-acetonylidene protected molecule **10g** was partially blocked by the "gate" (Fig. 6c), the binding pose of **10g** is much more flat than **12b** in order to reach the same binding site as **12b**. These results demonstrated that the 2′-methoxy group plays an important role in the binding of these small molecules to FXR.

These modelling results are interesting in that the putative binding positions of **10b** (14β) and **12g** (14β), and the putative orientations of decalin rings of **12b** (14β) and **10g** (14β) are similar to those of **5** (14α) but not of **6** (14β), respectively.

Conclusions

In summary, starting from the readily available natural compound of andrographolide (**1**), a series of andrographolide derivatives by the introduction of various substituted phenoxy groups to andrographolide at 14-position were straightforwardly synthesized with inversion of the 14-configuration by the Mitsunobu reaction. Our primary SAR studies revealed that 14-phenoxy andrographolide scaffold is an excellent structural moiety for FXR antagonists. Structural tuning of the substitutions at 14-phenoxy, modifications at 3,19-positions and 14-configurations could be an efficient way to discover 14-phenoxy andrographolide derivatives as effective FXR antagonists with low cellular toxicity. Remarkably, 14β-compounds of **12b**,

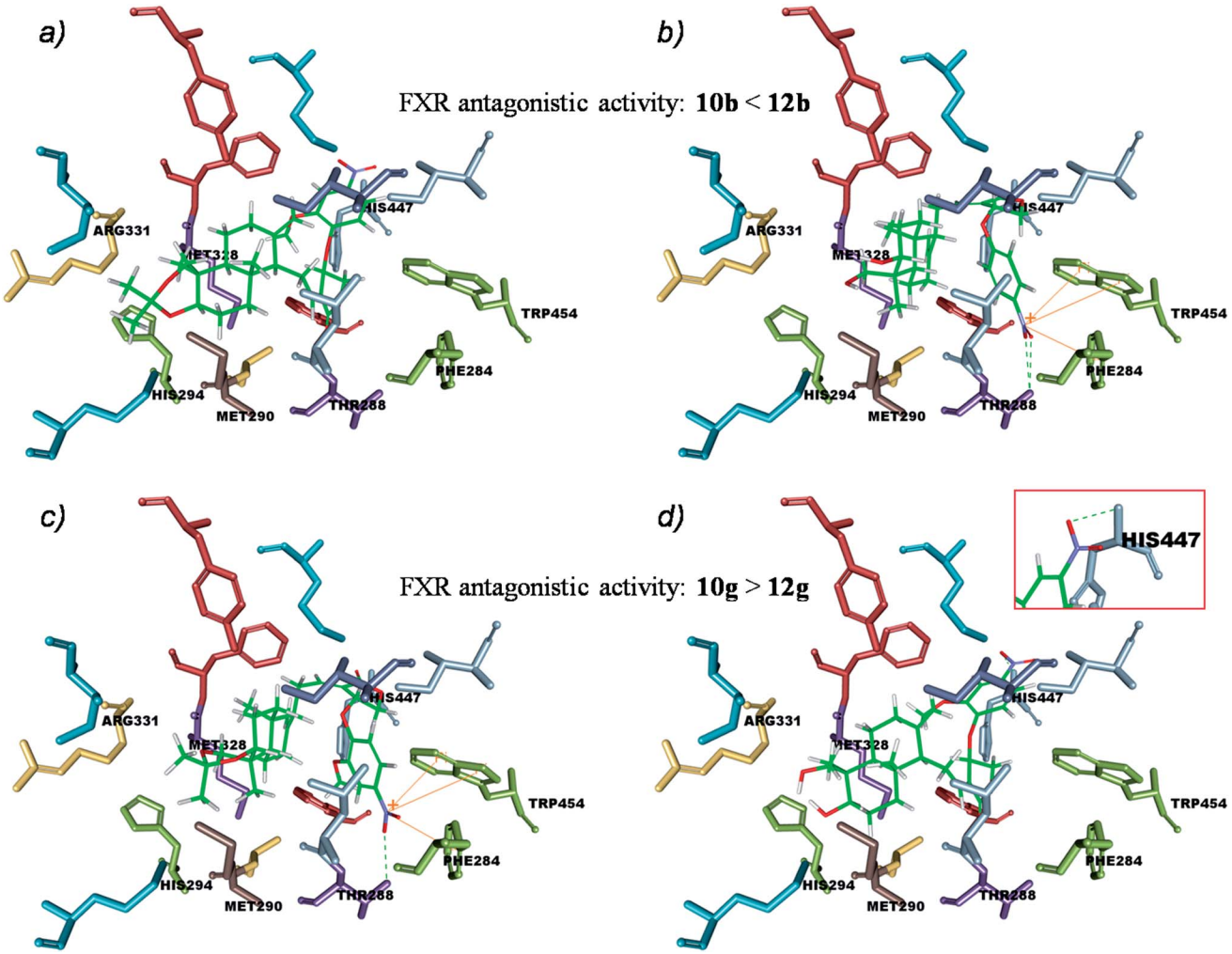

Fig. 6 Three-dimensional (3D) interaction diagrams of predicted binding positions of **10b** (a), **12b** (b), **10g** (c) and **12g** (d) in FXR active site. Critical amino acid residues of the binding pocket are labelled. The green dash line denotes hydrogen bonding between ligand and amino acid residue atoms of FXR protein, while the orange line denotes π–π interaction from the ligand to amino acid aromatic ring residue of the FXR protein. The inset (in red rectangle) of the hydrogen bond in **12g** (d) was viewed from a different visual angle.

12f and **10g** were found to be the most potent FXR antagonists in this work. Lesser stability and relatively weaker potency with somewhat cellular toxicity of α-isomers restricted their application in our current data. The structural docking unveiled that the structural features of a small FXR ligand affects its binding position, resulting in its FXR antagonistic discrepancy. It should be mentioned that these compounds have the potential to be optimized and developed into drug-like candidates in the future even compounds **6**, **10b–h**, **11b**, **11g** and **12h** have too high C Log *P* values (>5.0) to obey the Lipinski rule of 5. Taken together, the data strongly supports that andrographolide backbone combined with phenoxy substitution at the 14-position provides an excellent scaffold for FXR antagonists.

Experimental

Materials and equipment

Unless otherwise noted, materials were obtained from commercial suppliers and used without further purification. Melting points were measured using an YRT-3 melting point apparatus (Shanghai, China) and were uncorrected. ^{1}H and ^{13}C NMR spectra were recorded on a Bruker AV-400 spectrometer at 400 and 100 MHz, respectively, in $CDCl_3$, CD_3OD, DMSO-d_6, *etc.* as indicated. Coupling constants (*J*) are expressed in Hertz (Hz). Chemical shifts (δ) of NMR are reported in parts per million (ppm) units relative to the solvent. The low or high resolution of ESIMS (in the positive ion or negative ion acquisition mode) was recorded on an Agilent 1200 HPLC-MSD mass spectrometer or Applied Biosystems Q-STAR Elite ESI-LC-MS/MS mass spectrometer, respectively.

Preparation of 3,19-acetonylidene andrographolide (5)[36–38]

To the solution of 10 g (28.5 mmol) of andrographolide (**1**) and 24 ml (196 mmol) of 2,2-dimethoxypropane in 20.0 ml of anhydrous dichloromethane, 0.72 g (2.9 mmol) of PPTS was added and the reaction mixture was heated at 40 °C. The reaction was monitored by TLC and then treated with ethyl acetate and sat. $NaHCO_3$ after the reaction was complete. The organic

phase was washed with brine, dried over anhydrous Na_2SO_4, and then filtered organic solution was evaporated to dryness. The residue was purified by silica gel column chromatography (petroleum ether/ethyl acetate 1/1) to afford a white solid 10.05 g (90.2%); mp 187–192 °C. ^{1}H NMR (400 MHz, DMSO-d_6) δ 6.63 (t, J = 6.4 Hz, 1H), 5.74 (d, J = 6.0 Hz, 1H), 4.93 (t, J = 5.8 Hz, 1H), 4.86 (s, 1H), 4.69 (s, 1H), 4.41 (dd, J = 10.0, 6.0 Hz, 1H), 4.04 (dd, J = 9.8, 1.8 Hz, 1H), 3.89 (d, J = 11.6 Hz, 1H), 3.42 (dd, J = 9.2, 3.6 Hz, 1H), 3.12 (d, J = 11.6 Hz, 1H), 2.54–2.50 (m, 1H), 2.40–1.88 (m, 3H), 1.78–1.63 (m. 3H), 1.34 (s, 3H), 1.26 (s, 3H), 1.34–1.15 (m, 3H), 1.14 (s, 3H), 0.88 (s, 3H).

Preparation of 3,19-acetonylidene-14β-acetoxy-andrographolide (6)

Under N_2 atmosphere, 1.0 mmol of compound **5**, 1.5 mmol of PPh_3, 1.5 mmol of acetic acid were dissolved in 10.0 ml of anhydrous THF. The solution was cooled to 0 °C and then treated with 1.5 mmol of DIAD in 2.0 ml of anhydrous THF. The reaction was stirred overnight at room temperature after being stirred at 0 °C for 1 h. After distilling off the volatile solvents, the residue was dissolved in ethyl acetate and washed with brine about 5 times and dried over anhydrous Na_2SO_4. The filtered organic solution was evaporated to dryness and the residue was purified by silica gel column chromatography (petroleum ether–ethyl acetate 1 : 1) to give **6** (61%) as a white solid; mp 140–142 °C. ^{1}H NMR (400 MHz, C_6D_6) δ 7.00 (dd, J = 7.1, 1.8 Hz, 1H), 5.93 (dd, J = 5.6, 2.5 Hz, 1H), 4.89–4.84 (m, 1H), 4.56 (dd, J = 11.3, 6.2 Hz, 1H), 4.41 (d, J = 1.7 Hz, 1H), 4.22 (dd, J = 11.3, 1.9 Hz, 1H), 3.94 (d, J = 11.6 Hz, 1H), 3.49 (dd, J = 8.4, 3.9 Hz, 1H), 3.16 (d, J = 11.6 Hz, 1H), 2.55–2.31 (m, 3H), 2.10 (s, 3H), 1.98 (dd, J = 12.2, 6.4 Hz, 2H), 1.91–1.83 (m, 1H), 1.83–1.64 (m, 3H), 1.39 (s, 3H), 1.35 (s, 3H), 1.28 (tdd, J = 12.5, 8.2, 4.6 Hz, 3H), 1.18 (s, 3H), 0.94 (s, 3H); ^{13}C NMR (101 MHz, C_6D_6) δ 168.7, 161.3, 152.0, 146.9, 142.5, 126.4, 123.9, 115.3, 108.3, 80.3, 77.3, 71.8, 70.3, 64.0, 55.7, 55.2, 42.8, 39.0, 37.7, 36.9, 28.1, 25.8, 23.7, 22.7, 15.1; ESI-HRMS: m/z 455.2397 $[M + Na]^+$, calcd for $C_{25}H_{36}NaO_6$, 455.2410.

Preparation of 14β-acetoxy-andrographolide (7)

0.5 mmol of compound **6** was dissolved in 4 ml of methanol and then treated with 0.05 mmol of TsOH at 20 °C for 30 min. Diluted by ethyl acetate and washed with sat. $NaHCO_3$, brine, the organic phase was dried over anhydrous Na_2SO_4, filtered, evaporated by a rotavap to dryness. Compound **7** was purified by silica gel column chromatography (petroleum ether–ethyl acetate 10 : 7) (white solid, 93%, mp 163–165 °C). ^{1}H NMR (400 MHz, $CDCl_3$) δ 6.98 (dd, J = 7.0, 1.8 Hz, 1H), 5.91 (dt, J = 6.0, 1.8 Hz, 1H), 4.85 (q, J = 1.3 Hz, 1H), 4.54 (dd, J = 11.3, 6.1 Hz, 1H), 4.36 (d, J = 1.7 Hz, 1H), 4.20 (ddd, J = 25.9, 11.0, 1.8 Hz, 2H), 3.46 (dt, J = 10.2, 4.6 Hz, 1H), 3.36–3.26 (m, 1H), 3.00–2.89 (m, 2H), 2.53–2.26 (m, 3H), 2.11 (s, 3H), 1.96 (td, J = 12.5, 5.0 Hz, 1H), 1.89–1.75 (m, 4H), 1.75–1.68 (m, 1H), 1.36–1.12 (m, 6H), 0.66 (s, 3H); ^{13}C NMR (101 MHz, $CDCl_3$) δ 170.5, 169.1, 150.6, 146.8, 123.9, 108.4, 80.4, 71.7, 68.1, 64.1, 55.7, 55.2, 42.9, 39.0, 37.7, 36.9, 28.2, 28.2, 25.6, 23.7, 22.7, 20.8, 15.2; ESI-HRMS: m/z 415.2067 $[M + Na]^+$, calcd for $C_{22}H_{32}NaO_6$, 415.2097.

Preparation of 14β-andrographolide (8)

0.5 mmol of compound **6** was dissolved in 4 ml of methanol and then treated with 0.05 mmol of TsOH at 40–50 °C for 4 h. Diluted by ethyl acetate and washed with sat. $NaHCO_3$, brine, the organic phase was dried over anhydrous Na_2SO_4, filtered, evaporated by a rotavap to dryness. Compound **8** was purified by silica gel column chromatography (dichloromethane–ethyl acetate 1 : 2) (white solid, 80%, mp 200–202 °C). ^{1}H NMR (400 MHz, DMSO-d_6) δ 6.61 (ddd, J = 7.9, 6.1, 1.8 Hz, 1H), 5.64 (d, J = 6.1 Hz, 1H), 5.06 (d, J = 4.8 Hz, 1H), 4.94 (t, J = 6.1 Hz, 1H), 4.79 (d, J = 1.8 Hz, 1H), 4.45–4.36 (m, 2H), 4.12 (dd, J = 7.6, 2.8 Hz, 1H), 4.02 (dd, J = 9.9, 2.2 Hz, 1H), 3.84 (dd, J = 10.9, 2.9 Hz, 1H), 3.24 (ddd, J = 14.8, 9.9, 6.1 Hz, 2H), 2.63–2.53 (m, 1H), 2.43–2.26 (m, 2H), 1.92 (t, J = 12.2 Hz, 2H), 1.79–1.59 (m, 4H), 1.43–1.15 (m, 3H), 1.08 (s, 3H), 0.66 (s, 3H); ^{13}C NMR (101 MHz, C_6D6) δ 175.2, 153.3, 151.8, 134.5, 113.0, 83.8, 79.6, 70.2, 68.0, 60.7, 59.8, 47.6, 44.1, 42.9, 41.8, 33.2, 29.8, 29.3, 28.4, 20.2; ESI-HRMS: m/z 373.1981 $[M + Na]^+$, calcd for $C_{20}H_{30}NaO_5$, 373.1991.

Preparation of 3,19-acetonylidene-14β-andrographolide (9)

The same procedure was used as the preparation of compound **5**. The compound **9** was purified by silica gel column with petroleum ether/ethyl acetate 10/7 as a white solid (90%), mp 167–168 °C. ^{1}H NMR (400 MHz, $CDCl_3$) δ 6.95 (ddd, J = 8.0, 6.5, 1.8 Hz, 1H), 5.08 (t, J = 6.5 Hz, 1H), 4.87 (t, J = 1.5 Hz, 1H), 4.47 (dd, J = 10.5, 6.1 Hz, 1H), 4.43 (q, J = 1.3 Hz, 1H), 4.25 (dd, J = 10.5, 2.1 Hz, 1H), 3.96 (d, J = 11.6 Hz, 1H), 3.50 (dd, J = 8.6, 3.6 Hz, 1H), 3.18 (d, J = 11.6 Hz, 1H), 2.72–2.61 (m, 1H), 2.54–2.44 (m, 1H), 2.41 (dt, J = 13.3, 2.9 Hz, 1H), 2.07 (d, J = 6.8 Hz, 1H), 2.05–1.89 (m, 3H), 1.85–1.70 (m, 3H), 1.41 (s, 3H), 1.37 (s, 3H), 1.36–1.24 (m, 3H), 1.21 (s, 3H), 0.96 (s, 3H); ^{13}C NMR (101 MHz, DMSO) δ 169.8, 147.8, 146.3, 129.2, 108.1, 98.2, 75.8, 74.2, 64.8, 62.8, 55.2, 51.5, 38.2, 37.2, 37.1, 33.8, 27.4, 25.8, 25.2, 24.8, 24.6, 22.7, 15.8; ESI-HRMS: m/z 413.2302 $[M + Na]^+$, calcd for $C_{23}H_{34}NaO_5$, 413.2304.

Preparation of the series compounds 10a–10i, 11b and 11g

The same procedure was used as the preparation of 3,19-acetonylidene 14β-acetoxy andrographolide (**6**). Generally, the purification was conducted by silica gel column chromatography with petroleum ether–ethyl acetate from 3 : 1 to 1 : 1.

3,19-Acetonylidene-14β-phenoxy-andrographolide (10a)

From **5** in 51% yield, white solid, mp 153–155 °C. ^{1}H NMR (400 MHz, $CDCl_3$) δ (ppm) 7.39–7.28 (m, 2H), 7.13 (td, J = 7.4, 1.8 Hz, 1H), 7.05 (tt, J = 7.5, 1.0 Hz, 1H), 6.88–6.80 (m, 2H), 5.53 (d, J = 5.7 Hz, 1H), 4.87 (d, J = 1.6 Hz, 1H), 4.60 (dd, J = 10.7, 5.8 Hz, 1H), 4.46 (s, 1H), 4.40 (dd, J = 10.7, 2.0 Hz, 1H), 3.91 (d, J = 11.6 Hz, 1H), 3.42 (dd, J = 8.3, 3.9 Hz, 1H), 3.14 (d, J = 11.5 Hz, 1H), 2.57–2.46 (m, 1H), 2.45–2.26 (m, 2H), 1.95 (dd, J = 27.6, 12.1 Hz, 2H), 1.88–1.77 (m, 1H), 1.75–1.67 (m, 1H), 1.64 (dd, J = 11.8, 6.0 Hz, 1H), 1.51 (dd, J = 8.0, 5.4 Hz, 1H), 1.37 (s, 3H), 1.34 (s, 3H), 1.31–1.19 (m, 3H), 1.17 (s, 3H), 0.87 (s, 3H); ^{13}C NMR (101 MHz, C_6D_6) δ 168.8, 157.0, 149.6, 148.1, 130.1, 126.0, 122.2, 115.9, 108.0, 99.4, 75.4, 71.5, 70.5, 64.2, 55.8, 51.3, 38.5, 38.3, 37.8,

33.7, 26.7, 26.1, 25.7, 25.3, 24.8, 23.3, 16.6; ESI-HRMS: *m*/*z* 489.2658 $[M + Na]^+$, calcd for $C_{29}H_{38}NaO_5$, 489.2617.

3,19-Acetonylidene-14β-(4′-nitro-phenoxy)-andrographolide (10b)

From **5** in 52% yield, white solid, mp 179–181 °C. ^{1}H NMR (400 MHz, $CDCl_3$) δ 8.31–8.22 (m, 2H), 7.19 (ddd, J = 8.0, 6.7, 1.7 Hz, 1H), 6.97–6.88 (m, 2H), 5.69–5.62 (m, 1H), 4.89 (dd, J = 1.8, 1.0 Hz, 1H), 4.67 (dd, J = 10.9, 5.8 Hz, 1H), 4.45 (d, J = 1.5 Hz, 1H), 4.37 (dd, J = 10.9, 1.9 Hz, 1H), 3.88 (d, J = 11.6 Hz, 1H), 3.44 (dd, J = 7.8, 3.8 Hz, 1H), 3.14 (d, J = 11.5 Hz, 1H), 2.54 (ddd, J = 15.9, 7.8, 2.5 Hz, 1H), 2.47–2.31 (m, 2H), 2.04–1.89 (m, 2H), 1.85–1.75 (m, 1H), 1.75–1.68 (m, 1H), 1.68–1.59 (m, 1H), 1.51 (td, J = 8.0, 4.2 Hz, 1H), 1.35 (s, 3H), 1.33 (s, 3H), 1.31–1.21 (m, 3H), 1.16 (s, 3H), 0.89 (s, 3H); ^{13}C NMR (101 MHz, $CDCl_3$) δ 168.68, 161.28, 151.98, 147.27, 142.53, 126.35, 123.93, 115.16, 108.26, 99.37, 75.42, 71.78, 70.26, 64.05, 55.82, 51.66, 38.50, 38.10, 37.58, 33.85, 26.47, 26.01, 25.94, 25.10, 24.43, 23.17, 16.44; ESI-HRMS: *m*/*z* 534.2473 $[M + Na]^+$, calcd for $C_{29}H_{37}NNaO_7$, 534.2468.

3,19-Acetonylidene-14β-(3′-nitro-phenoxy)-andrographolide (10c)

From **5** in 32% yield, white solid, mp 163–165 °C. ^{1}H NMR (400 MHz, C_6D_6) δ 7.51 (d, J = 7.1 Hz, 1H), 7.31 (d, J = 2.1 Hz, 1H), 7.23–7.16 (m, 1H), 6.62 (t, J = 8.2 Hz, 1H), 6.52 (dd, J = 8.3, 1.8 Hz, 1H), 4.85 (s, 1H), 4.62 (d, J = 5.1 Hz, 1H), 4.43 (s, 1H), 3.77 (d, J = 11.6 Hz, 1H), 3.67–3.54 (m, 2H), 3.41 (dd, J = 7.1, 3.5 Hz, 1H), 3.06 (d, J = 11.5 Hz, 1H), 2.12 (ddd, J = 22.8, 17.7, 9.7 Hz, 3H), 1.68 (dt, J = 13.0, 6.6 Hz, 2H), 1.53–1.36 (m, 2H), 1.39 (s, 3H), 1.35–1.25 (m, 2H), 1.34 (s, 3H), 1.07 (s, 3H), 0.99 (td, J = 13.0, 3.8 Hz, 1H), 0.94–0.80 (m, 2H), 0.84 (s, 3H); ^{13}C NMR (101 MHz, C_6D_6) δ 168.1, 157.1, 150.2, 149.5, 147.8, 130.4, 124.9, 122.2, 116.8, 109.2, 108.0, 99.5, 74.9, 71.8, 69.8, 64.2, 55.6, 51.0, 38.4, 38.2, 37.6, 33.5, 26.2, 25.9, 25.8, 25.1, 24.4, 23.1, 16.6; ESI-HRMS: *m*/*z* 534.2463 $[M + Na]^+$, calcd for $C_{29}H_{37}NNaO_7$, 534.2468.

3,19-Acetonylidene-14β-(2′-nitro-phenoxy)-andrographolide (10d)

From **5** in 73% yield, white solid, mp 146–148 °C. ^{1}H NMR (400 MHz, C_6D_6) δ 7.27 (dd, J = 8.0, 1.7 Hz, 1H), 7.21 (ddd, J = 8.1, 6.3, 1.9 Hz, 1H), 6.77–6.65 (m, 1H), 6.34 (td, J = 7.8, 1.1 Hz, 1H), 6.06–5.92 (m, 1H), 4.93–4.80 (m, 2H), 4.38 (t, J = 2.8 Hz, 1H), 3.82 (d, J = 11.5 Hz, 1H), 3.60 (qd, J = 10.8, 4.2 Hz, 2H), 3.45 (dd, J = 7.7, 3.3 Hz, 1H), 3.08 (d, J = 11.5 Hz, 1H), 2.40–2.29 (m, 1H), 2.26–2.11 (m, 2H), 1.86–1.67 (m, 2H), 1.62–1.47 (m, 3H), 1.42 (s, 3H), 1.36 (s, 3H), 1.36–1.31 (m, 1H), 1.12 (s, 3H), 1.05–0.91 (m, 3H), 0.87 (s, 3H); ^{13}C NMR (101 MHz, C_6D_6) δ 168.0, 151.6, 149.3, 148.4, 141.6, 133.2, 127.7, 125.8, 124.3, 121.7, 115.8, 107.8, 99.3, 75.4, 73.3, 69.6, 64.1, 55.7, 51.0, 38.4, 38.1, 37.6, 33.6, 26.7, 25.9, 25.2, 24.7, 23.2, 16.5; ESI-HRMS: *m*/*z* 534.2467 $[M + Na]^+$, calcd for $C_{29}H_{37}NNaO_7$, 534.2468.

Ethyl 3,19-acetonylidene-14β-(2′-carboxy-phenoxy)-andrographolide (10e)

From **5** in 78% yield, white solid, mp 168–170 °C. ^{1}H NMR (400 MHz, C_6D_6) δ 7.80 (dd, J = 7.7, 1.8 Hz, 1H), 7.24–7.18 (m, 1H), 6.98–6.92 (m, 1H), 6.69 (td, J = 7.6, 0.9 Hz, 1H), 6.28 (d, J = 8.2 Hz, 1H), 5.04 (d, J = 5.4 Hz, 1H), 4.87–4.81 (m, 1H), 4.44 (s, 1H), 4.12 (qq, J = 10.9, 7.1 Hz, 2H), 4.01 (dd, J = 10.6, 1.4 Hz, 1H), 3.82 (d, J = 11.5 Hz, 1H), 3.68 (dd, J = 10.6, 5.5 Hz, 1H), 3.42 (dd, J = 7.6, 3.7 Hz, 1H), 3.08 (d, J = 11.5 Hz, 1H), 2.24–2.05 (m, 3H), 1.73 (dq, J = 13.4, 6.8 Hz, 2H), 1.59 (d, J = 8.3 Hz, 1H), 1.53–1.43 (m, 1H), 1.43–1.31 (m, 2H), 1.41 (s, 3H), 1.37 (s, 3H), 1.11 (s, 3H), 1.04 (t, J = 7.1 Hz, 3H), 1.01–0.89 (m, 3H), 0.85 (s, 3H); ^{13}C NMR (101 MHz, C_6D_6) δ 168.7, 165.7, 156.0, 149.7, 148.2, 132.9, 132.2, 127.8, 125.8, 123.9, 122.2, 116.6, 107.9, 99.3, 75.3, 73.2, 70.3, 64.1, 61.0, 55.8, 51.0, 38.4, 38.2, 37.6, 33.5, 26.6, 25.9[1], 25.8[7], 25.2, 24.6, 23.2, 16.5, 14.1; ESI-HRMS: *m*/*z* 561.2829 $[M + Na]^+$, calcd for $C_{32}H_{42}NaO_7$, 561.2828.

3,19-Acetonylidene-14β-(2′-methoxy-phenoxy)-andrographolide (10f)

From **5** in 60% yield, white solid, mp 130–131 °C. ^{1}H NMR (400 MHz, C_6D_6) δ 7.13–7.10 (m, 1H), 6.80 (td, J = 7.8, 1.7 Hz, 1H), 6.65 (td, J = 7.7, 1.5 Hz, 1H), 6.58 (dd, J = 7.9, 1.6 Hz, 1H), 6.47 (dd, J = 8.1, 1.3 Hz, 1H), 5.18 (d, J = 5.4 Hz, 1H), 4.82 (d, J = 1.2 Hz, 1H), 4.42 (s, 1H), 4.15 (dd, J = 10.6, 1.5 Hz, 1H), 3.83 (d, J = 11.5 Hz, 1H), 3.65 (dd, J = 10.6, 5.5 Hz, 1H), 3.41 (dd, J = 7.7, 3.7 Hz, 1H), 3.29 (s, 3H), 3.09 (d, J = 11.5 Hz, 1H), 2.26–2.04 (m, 3H), 1.83–1.62 (m, 2H), 1.54–1.28 (m, 10H), 1.08 (s, 3H), 1.05–0.82 (m, 6H); ^{13}C NMR (101 MHz, C_6D_6) δ 169.08, 151.78, 149.42, 148.27, 145.92, 128.15, 128.03, 127.91, 127.79, 127.67, 126.39, 124.00, 121.11, 120.16, 112.54, 107.85, 99.30, 75.39, 73.44, 70.56, 64.14, 55.72, 55.11, 51.10, 38.34, 38.12, 37.66, 33.56, 26.57, 26.00, 25.64, 25.29, 24.74, 23.24, 16.46; ESI-HRMS: *m*/*z* 519.2715 $[M + Na]^+$, calcd for $C_{30}H_{40}NaO_6$, 519.2723.

3,19-Acetonylidene-14β-(2′-methoxy-4′-nitro-phenoxy)-andrographolide (10g)

From **5** in 51% yield, pale yellowish solid, mp 129–131 °C. ^{1}H NMR (400 MHz, C_6D_6) δ 7.56 (dd, J = 8.8, 2.6 Hz, 1H), 7.46 (d, J = 2.6 Hz, 1H), 7.20–7.15 (m, 1H), 5.95 (d, J = 8.8 Hz, 1H), 4.88 (d, J = 5.5 Hz, 1H), 4.83 (d, J = 1.5 Hz, 1H), 4.41–4.37 (m, 1H), 3.82–3.74 (m, 2H), 3.60 (dd, J = 10.8, 5.7 Hz, 1H), 3.41 (dd, J = 7.3, 3.6 Hz, 1H), 3.08 (s, 1H), 3.05 (s, 3H), 2.19–2.10 (m, 3H), 1.77–1.60 (m, 2H), 1.52–1.44 (m, 1H), 1.44–1.36 (m, 1H), 1.40 (s, 3H), 1.36 (s, 3H), 1.34–1.25 (m, 2H), 1.06 (s, 3H), 1.03–0.93 (m, 1H), 0.94–0.80 (m, 3H), 0.85 (s, 3H); ^{13}C NMR (101 MHz, C_6D_6) δ 168.1, 150.8, 150.5, 150.3, 148.1, 143.2, 124.9, 116.9, 115.0, 107.7, 107.1, 99.4, 74.8, 72.9, 69.7, 64.0, 55.4, 55.1, 50.7, 38.2, 38.1, 37.4, 33.2, 26.1, 25.8, 25.6, 25.0, 24.3, 23.0, 16.4; ESI-HRMS: *m*/*z* 564.2584 $[M + Na]^+$, calcd for $C_{30}H_{39}NNaO_8$, 564.2573.

3,19-Acetonylidene-14β-(2′-methyl-4′-nitro-phenoxy)-andrographolide (10h)

From **5** in 61% yield, white solid, mp 168–170 °C. ^{1}H NMR (400 MHz, C_6D_6) δ 8.13 (d, J = 7.7 Hz, 2H), 7.19 (td, J = 7.2, 1.7 Hz, 1H), 6.79–6.70 (m, 1H), 5.67 (d, J = 5.6 Hz, 1H), 4.91–4.84 (m, 1H), 4.67 (dd, J = 10.9, 5.7 Hz, 1H), 4.43 (d, J = 1.8 Hz, 1H), 4.35 (dd, J = 11.0, 1.7 Hz, 1H), 3.87 (d, J = 11.6 Hz, 1H), 3.43 (dd, J = 7.7, 3.7 Hz, 1H), 3.13 (d, J = 11.6 Hz, 1H), 2.51 (ddd, J = 16.2, 7.4, 2.6 Hz, 1H), 2.45–2.34 (m, 2H), 2.27 (s, 3H), 1.96 (ddd, J = 27.0,

12.4, 6.9 Hz, 2H), 1.83–1.66 (m, 2H), 1.65–1.44 (m, 3H), 1.34 (s, 3H), 1.33 (s, 3H), 1.31–1.17 (m, 3H), 1.15 (s, 3H), 0.89 (s, 3H); ^{13}C NMR (101 MHz, C_6D_6) δ 162.6, 153.7, 145.2, 142.7, 136.9, 123.1, 121.4, 119.4, 117.9, 105.4, 102.5, 94.2, 69.1, 66.5, 64.3, 58.8, 50.5, 45.4, 32.9, 32.2, 27.9, 20.5, 19.6, 18.7, 17.7, 11.4, 10.5; ESI-HRMS: m/z 548.2636 $[M + Na]^+$, calcd for $C_{30}H_{39}NNaO_7$, 548.2624.

3,19-Acetonylidene-14β-(2′-fluoro-4′-nitro-phenoxy)-andrographolide (10i)

From **5** in 72% yield, white solid, mp 114–117 °C. ^{1}H NMR (400 MHz, C_6D_6) δ 7.56 (dd, J = 10.6, 2.6 Hz, 1H), 7.47 (ddd, J = 9.1, 2.7, 1.5 Hz, 1H), 7.23–7.18 (m, 1H), 5.75 (td, J = 8.4, 3.3 Hz, 1H), 4.84 (d, J = 1.8 Hz, 1H), 4.70 (d, J = 5.1 Hz, 1H), 4.39 (d, J = 1.7 Hz, 1H), 3.77 (d, J = 11.6 Hz, 1H), 3.63–3.51 (m, 2H), 3.43 (dd, J = 7.0, 3.5 Hz, 1H), 3.05 (d, J = 11.5 Hz, 1H), 2.26–2.08 (m, 3H), 1.79–1.60 (m, 2H), 1.55–1.43 (m, 2H), 1.39 (s, 3H), 1.34 (s, 3H), 1.36–1.27 (m, 2H), 1.05 (s, 3H), 1.01–0.85 (m, 3H), 0.89 (s, 3H); ^{13}C NMR (101 MHz, C_6D_6) δ 167.9, 167.7, 153.1, 151.5, 151.4, 150.6, 149.7, 149.6, 148.17, 142.3, 142.3, 124.2, 120.6, 115.0, 113.0, 112.8, 107.8, 99.5, 74.7, 73.4, 69.5, 64.2, 55.5, 50.7, 38.3, 38.3, 37.5, 33.2, 26.0, 25.8 (2C), 25.0, 24.2, 23.1, 16.7; ESI-HRMS: m/z 552.2418 $[M + Na]^+$, calcd for $C_{29}H_{36}FNNaO_7$, 552.2374.

3,19-Acetonylidene-14α-(4′-nitro-phenoxy)-andrographolide (11b)

From **9** in 56% yield, white solid, mp 149–152 °C. ^{1}H NMR (400 MHz, Benzene-d_6) δ 7.80–7.74 (m, 2H), 6.39 (dd, J = 9.5, 2.4 Hz, 2H), 6.11 (dt, J = 4.7, 1.9 Hz, 1H), 5.49 (s, 1H), 5.20 (dt, J = 10.7, 1.8 Hz, 1H), 5.17–5.13 (m, 1H), 3.86 (d, J = 11.5 Hz, 1H), 3.68 (dd, J = 3.3, 2.0 Hz, 2H), 3.50 (dd, J = 7.1, 3.4 Hz, 1H), 3.09 (d, J = 11.5 Hz, 1H), 2.36–2.20 (m, 2H), 2.09–2.03 (m, 1H), 2.02–1.92 (m, 1H), 1.85 (dd, J = 14.6, 10.6 Hz, 1H), 1.81–1.63 (m, 3H), 1.51 (dd, J = 12.6, 6.7 Hz, 1H), 1.43 (s, 3H), 1.41 (s, 3H), 1.33 (ddt, J = 6.9, 5.1, 2.9 Hz, 1H), 1.12–0.97 (m, 2H), 1.03 (s, 3H), 1.02 (s, 3H); ^{13}C NMR (101 MHz, C_6D_6) δ 171.5, 162.4, 147.2, 145.7, 142.2, 134.0, 125.9, 115.0, 109.1, 99.5, 75.0, 73.0, 69.9, 64.3, 52.3, 51.4, 38.4, 38.3, 38.2, 33.9, 30.9, 26.2, 25.8, 25.2, 24.6, 23.4, 17.0; ESI-HRMS: m/z 534.2500 $[M + Na]^+$, calcd for $C_{29}H_{37}NNaO_7$, 534.2468.

3,19-Acetonylidene-14α-(2′-methoxy-4′-nitro-phenoxy)-andrographolide (11g)

From **9** in 50% yield, white solid, mp 121–123 °C. ^{1}H NMR (400 MHz, C_6D_6) δ 7.56 (dd, J = 8.8, 2.4 Hz, 1H), 7.45 (d, J = 2.5 Hz, 1H), 7.14–7.10 (m, 1H), 6.07–5.99 (m, 1H), 4.90 (s, 1H), 4.82 (s, 1H), 4.61 (s, 1H), 3.81 (dd, J = 13.3, 6.7 Hz, 2H), 3.71 (dd, J = 10.8, 5.9 Hz, 1H), 3.46 (dd, J = 7.5, 3.7 Hz, 1H), 3.07 (t, J = 6.6 Hz, 4H), 2.41–2.24 (m, 1H), 2.22–2.05 (m, 2H), 1.85 (td, J = 13.6, 6.4 Hz, 1H), 1.79–1.67 (m, 1H), 1.62–1.52 (m, 1H), 1.52–1.28 (m, 9H), 1.06 (d, J = 16.4 Hz, 3H), 1.04–0.89 (m, 3H), 0.84–0.74 (m, 3H); ^{13}C NMR (101 MHz, C_6D_6) δ 168.17, 151.11, 150.60, 147.17, 143.51, 124.80, 116.98, 115.61, 109.33, 107.40, 99.44, 75.17, 73.37, 69.90, 64.12, 55.82, 55.21, 51.25, 38.16, 38.04, 37.64, 34.06, 26.32, 26.01, 25.32, 25.20, 24.69, 23.16, 16.39; ESI-HRMS: m/z 564.2569 $[M + Na]^+$, calcd for $C_{30}H_{39}NNaO_8$, 564.2573.

Preparation of the series compounds 12a–12i, 13b and 13g

The same procedure was used as the preparation of compound **7**. Generally, the purification was conducted by silica gel column chromatography with petroleum ether–ethyl acetate from 2 : 1 to 1 : 1.

14β-Phenoxy-andrographolide (12a)

From **10a** in 86% yield, white solid, mp 164–166 °C. ^{1}H NMR (400 MHz, $CDCl_3$) δ 7.40–7.29 (m, 2H), 7.14–7.01 (m, 2H), 6.89–6.79 (m, 2H), 5.55–5.48 (m, 1H), 4.85 (dd, J = 1.9, 1.0 Hz, 1H), 4.60 (dd, J = 10.7, 5.9 Hz, 1H), 4.44–4.36 (m, 2H), 4.17–4.08 (m, 1H), 3.40 (dd, J = 11.5, 4.3 Hz, 1H), 3.29 (d, J = 10.9 Hz, 1H), 2.54–2.44 (m, 1H), 2.44–2.36 (m, 1H), 2.33–2.23 (m, 1H), 2.16 (d, J = 26.3 Hz, 3H), 1.97 (td, J = 12.7, 10.7, 6.2 Hz, 1H), 1.92–1.85 (m, 1H), 1.85–1.70 (m, 2H), 1.70–1.55 (m, 2H), 1.33–1.16 (m, 5H), 1.11 (td, J = 13.5, 3.7 Hz, 1H), 0.58 (s, 3H); ^{13}C NMR (101 MHz, C_6D6) δ 169.5, 156.4, 150.8, 147.1, 130.0, 125.0, 122.3, 115.7, 108.2, 80.4, 71.3, 71.0, 64.1, 55.9, 55.1, 42.8, 39.0, 37.7, 36.8, 28.1, 25.6, 23.7, 22.7, 15.1; HRMS (ESI): m/z 449.2342 $[M + Na]^+$, calcd for $C_{26}H_{34}NaO_5$, 449.2304.

14β-(4′-Nitro-phenoxy)-andrographolide (12b)

From **10b** in 89% yield, white solid, mp 184–186 °C. ^{1}H NMR (400 MHz, $CDCl_3$) δ 8.32–8.23 (m, 2H), 7.18–7.11 (m, 1H), 6.93 (d, J = 9.2 Hz, 2H), 5.63 (d, J = 5.7 Hz, 1H), 4.87 (s, 1H), 4.67 (dd, J = 10.9, 5.8 Hz, 1H), 4.43–4.32 (m, 2H), 4.13 (d, J = 11.2 Hz, 1H), 3.42 (dd, J = 11.6, 4.3 Hz, 1H), 3.29 (d, J = 11.0 Hz, 1H), 2.50 (dd, J = 7.0, 2.7 Hz, 1H), 2.46–2.37 (m, 1H), 2.32 (dd, J = 10.7, 7.1 Hz, 1H), 2.05 (s, 3H), 1.97 (dd, J = 12.7, 5.2 Hz, 1H), 1.90 (d, J = 10.5 Hz, 1H), 1.87–1.70 (m, 2H), 1.70–1.63 (m, 1H), 1.60 (dd, J = 13.0, 3.5 Hz, 1H), 1.34–1.18 (m, 5H), 1.13 (td, J = 13.2, 3.8 Hz, 1H), 0.60 (s, 3H); ^{13}C NMR (101 MHz, $CDCl_3$) δ 168.7, 161.3, 152.0, 146.9, 142.5, 126.4, 123.9, 115.3, 108.3, 80.3, 77.3, 71.8, 70.3, 64.0, 55.7, 55.2, 42.8, 39.0, 37.7, 36.9, 28.1, 25.8, 23.7, 22.7, 15.1; HRMS (ESI): m/z 494.2148 $[M + Na]^+$, calcd for $C_{26}H_{33}NNaO_7$, 494.2155.

14β-(3′-nitro-phenoxy)-andrographolide (12c)

From **10c** in 92% yield, white solid, mp 144–146 °C. ^{1}H NMR (400 MHz, $CDCl_3$) δ 7.94 (ddd, J = 8.2, 2.0, 0.9 Hz, 1H), 7.69 (t, J = 2.3 Hz, 1H), 7.54 (t, J = 8.2 Hz, 1H), 7.20 (ddd, J = 8.3, 2.6, 0.9 Hz, 1H), 7.14 (td, J = 7.1, 1.7 Hz, 1H), 5.62 (dt, J = 5.6, 1.7 Hz, 1H), 4.87 (q, J = 1.3 Hz, 1H), 4.67 (dd, J = 10.9, 5.7 Hz, 1H), 4.45–4.35 (m, 2H), 4.12 (d, J = 11.2 Hz, 1H), 3.41 (ddd, J = 11.7, 4.5, 1.3 Hz, 1H), 3.29 (dd, J = 11.2, 1.3 Hz, 1H), 2.51 (ddd, J = 16.1, 7.2, 3.0 Hz, 1H), 2.46–2.38 (m, 1H), 2.37–2.23 (m, 4H), 1.98 (td, J = 12.6, 4.9 Hz, 1H), 1.93–1.87 (m, 1H), 1.87–1.79 (m, 1H), 1.79–1.69 (m, 1H), 1.62 (ddt, J = 24.2, 13.1, 3.8 Hz, 2H), 1.34–1.18 (m, 5H), 1.12 (td, J = 13.2, 4.1 Hz, 1H), 0.60 (s, 3H); ^{13}C NMR (101 MHz, $CDCl_3$) δ 168.9, 157.0, 151.7, 149.4, 146.9, 130.9, 124.2, 122.4, 117.3, 109.7, 108.3, 80.3, 71.9, 70.4, 64.1, 55.8, 55.2, 42.8, 39.00, 37.7, 36.9, 28.1, 25.7, 23.7, 22.7, 15.1; HRMS (ESI): m/z 494.2156 $[M + Na]^+$, calcd for $C_{26}H_{33}NNaO_7$, 494.2155.

14β-(2′-nitro-phenoxy)-andrographolide (12d)

From **10d** in 86% yield, white solid, mp 167–168 °C. ^{1}H NMR (400 MHz, $CDCl_3$) δ 7.89 (dd, J = 8.1, 1.6 Hz, 1H), 7.62–7.55 (m, 1H), 7.18 (t, J = 7.7 Hz, 1H), 7.15–7.10 (m, 1H), 6.92 (d, J = 8.3 Hz, 1H), 5.64 (d, J = 5.6 Hz, 1H), 4.83 (s, 1H), 4.66 (dd, J = 10.9, 6.0 Hz, 1H), 4.44 (dd, J = 10.9, 2.0 Hz, 1H), 4.31 (s, 1H), 4.13 (d, J = 11.2 Hz, 1H), 3.43 (dd, J = 11.5, 4.6 Hz, 1H), 3.28 (d, J = 11.1 Hz, 1H), 2.56–2.45 (m, 1H), 2.38 (dd, J = 13.2, 3.5 Hz, 1H), 2.26 (ddd, J = 16.5, 11.2, 7.8 Hz, 1H), 2.09 (s, 3H), 1.98 (t, J = 12.3 Hz, 1H), 1.89 (d, J = 10.4 Hz, 1H), 1.85–1.78 (m, 1H), 1.78–1.63 (m, 2H), 1.59 (dt, J = 13.0, 3.3 Hz, 1H), 1.24 (s, 5H), 1.10 (td, J = 13.2, 3.9 Hz, 1H), 0.58 (s, 3H); ^{13}C NMR (101 MHz, $CDCl_3$) δ 168.7, 152.6, 149.4, 147.3, 141.1, 134.1, 126.3, 123.7, 122.3, 115.9, 108.1, 80.3, 73.1, 70.3, 64.1, 55.8, 54.9, 42.8, 38.9, 37.6, 36.5, 28.1, 25.8, 23.7, 22.6, 15.1; HRMS (ESI): m/z 494.2158 $[M + Na]^+$, calcd for $C_{26}H_{33}NNaO_7$, 494.2155.

Ethyl 14β-(2′-carboxy-phenoxy)-andrographolide (12e)

From **10e** in 88% yield, white solid, mp 181–182 °C. ^{1}H NMR (400 MHz, $CDCl_3$) δ 7.88 (dd, J = 7.8, 1.7 Hz, 1H), 7.56–7.46 (m, 1H), 7.20–7.11 (m, 1H), 7.04 (ddd, J = 7.7, 6.0, 1.6 Hz, 1H), 6.91 (d, J = 8.3 Hz, 1H), 5.61 (d, J = 5.3 Hz, 1H), 4.83 (d, J = 1.9 Hz, 1H), 4.63–4.48 (m, 2H), 4.41–4.26 (m, 3H), 4.14 (d, J = 11.1 Hz, 1H), 3.41 (dt, J = 11.7, 2.8 Hz, 1H), 3.29 (d, J = 10.9 Hz, 1H), 2.47–2.25 (m, 4H), 2.17 (ddd, J = 16.4, 11.2, 8.2 Hz, 1H), 1.96 (td, J = 12.6, 5.2 Hz, 1H), 1.88–1.78 (m, 2H), 1.78–1.61 (m, 2H), 1.36 (t, J = 7.1 Hz, 3H), 1.32–1.16 (m, 5H), 1.04 (td, J = 13.3, 3.9 Hz, 1H), 0.56 (s, 3H); ^{13}C NMR (101 MHz, $CDCl_3$) δ 169.5, 165.7, 155.8, 150.9, 147.1, 133.4, 132.3, 124.9, 123.2, 122.6, 117.0, 108.2, 80.3, 73.4, 71.0, 64.1, 61.2, 55.8, 54.9, 42.8, 38.8, 37.6, 36.6, 28.1, 25.6, 23.7, 22.6, 15.1, 14.3; HRMS (ESI): m/z 521.2517 $[M + Na]^+$, calcd for $C_{29}H_{39}NaO_7$, 521.2515.

14β-(2′-methoxy-phenoxy)-andrographolide (12f)

From **10f** in 93% yield, white solid, mp 176–178 °C. ^{1}H NMR (400 MHz, $CDCl_3$) δ 7.13–7.02 (m, 1H), 7.01–6.83 (m, 4H), 5.58 (t, J = 13.3 Hz, 1H), 4.82 (t, J = 7.3 Hz, 1H), 4.55–4.40 (m, 2H), 4.32 (dd, J = 7.6, 6.7 Hz, 1H), 4.13 (t, J = 8.9 Hz, 1H), 3.92–3.81 (m, 3H), 3.47–3.35 (m, 1H), 3.30 (d, J = 11.1 Hz, 1H), 2.42–2.33 (m, 1H), 2.32–2.21 (m, 2H), 2.02–1.66 (m, 5H), 1.56 (dt, J = 13.3, 3.6 Hz, 1H), 1.31–1.02 (m, 6H), 0.61 (dd, J = 18.6, 2.5 Hz, 3H); ^{13}C NMR (101 MHz, $CDCl_3$) δ 169.77, 151.35, 150.68, 147.23, 145.29, 125.46, 124.33, 121.09, 119.97, 112.35, 108.12, 80.45, 73.42, 71.20, 64.14, 55.80, 55.69, 55.03, 42.87, 38.88, 37.69, 36.64, 28.22, 25.55, 23.73, 22.70, 15.10; HRMS (ESI): m/z 479.2408 $[M + Na]^+$, calcd for $C_{27}H_{36}NaO_6$, 479.2410.

14β-(2′-methoxy-4′-nitro-phenoxy)-andrographolide (12g)

From **10g** in 87% yield, pale yellowish solid, mp 151–153 °C. ^{1}H NMR (400 MHz, $CDCl_3$) δ 8.13 (d, J = 7.1 Hz, 2H), 7.16 (q, J = 7.0, 6.5 Hz, 1H), 6.75 (d, J = 9.6 Hz, 1H), 5.64 (d, J = 5.4 Hz, 1H), 4.86 (s, 1H), 4.67 (dd, J = 10.9, 5.7 Hz, 1H), 4.39–4.32 (m, 2H), 4.12 (d, J = 11.1 Hz, 1H), 3.39 (dd, J = 11.7, 4.3 Hz, 1H), 3.29 (d, J = 11.2 Hz, 1H), 2.54–2.38 (m, 2H), 2.31 (d, J = 32.5 Hz, 5H), 2.11 (s, 3H), 1.97 (dt, J = 13.0, 6.4 Hz, 1H), 1.92–1.77 (m, 2H), 1.78–1.68 (m, 1H), 1.68–1.60 (m, 1H), 1.57 (dd, J = 12.9, 3.3 Hz, 1H), 1.34–1.15 (m, 5H), 1.08 (td, J = 13.4, 3.6 Hz, 1H), 0.59 (s, 3H); ^{13}C NMR (101 MHz, $CDCl_3$) δ 169.0, 151.8, 151.0, 150.6, 147.1, 143.3, 124.4, 117.4, 116.0, 108.2, 107.5, 80.4, 73.3, 70.6, 64.0, 56.4, 55.7, 55.1, 42.8, 38.9, 37.6, 36.6, 28.2, 25.7, 23.7, 22.8, 15.1; HRMS (ESI): m/z 524.2254 $[M + Na]^+$, calcd for $C_{27}H_{35}NNaO_8$, 524.2260.

14β-(2′-methyl-4′-nitro-phenoxy)-andrographolide (12h)

From **10h** in 87% yield, white solid, mp 115–117 °C. ^{1}H NMR (400 MHz, $CDCl_3$) δ 8.13 (d, J = 7.7 Hz, 2H), 7.19 (td, J = 7.2, 1.7 Hz, 1H), 6.79–6.70 (m, 1H), 5.67 (d, J = 5.6 Hz, 1H), 4.91–4.84 (m, 1H), 4.67 (dd, J = 10.9, 5.7 Hz, 1H), 4.43 (d, J = 1.8 Hz, 1H), 4.35 (dd, J = 11.0, 1.7 Hz, 1H), 3.87 (d, J = 11.6 Hz, 1H), 3.43 (dd, J = 7.7, 3.7 Hz, 1H), 3.13 (d, J = 11.6 Hz, 1H), 2.51 (ddd, J = 16.2, 7.4, 2.6 Hz, 1H), 2.45–2.34 (m, 2H), 2.27 (s, 3H), 1.96 (ddd, J = 27.0, 12.4, 6.9 Hz, 2H), 1.83–1.66 (m, 2H), 1.65–1.44 (m, 3H), 1.33 (d, J = 6.2 Hz, 6H), 1.31–1.17 (m, 3H), 1.15 (s, 3H), 0.89 (s, 3H); ^{13}C NMR (101 MHz, $CDCl_3$) δ 168.7, 152.6, 149.3, 147.2, 141.0, 134.1, 126.2, 123.6, 122.3, 115.8, 108.0, 80.3, 73.1, 70.3, 64.1, 55.7, 54.8, 42.7, 38.8, 37.6, 36.5, 28.1, 25.8, 23.6, 22.6, 15.1; HRMS (ESI): m/z 508.2305 $[M + Na]^+$, calcd for $C_{27}H_{35}NNaO_7$, 508.2311.

14β-(2′-fluoro-4′-nitro-phenoxy)-andrographolide (12i)

From **10i** in 91% yield, white solid, mp 162–165 °C. ^{1}H NMR (400 MHz, CD_3OD) δ 8.20–8.12 (m, 2H), 7.35 (t, J = 8.4 Hz, 1H), 7.14–7.05 (m, 1H), 6.04–5.98 (m, 1H), 4.91 (s, 1H), 4.73 (dd, J = 11.2, 5.5 Hz, 1H), 4.57 (s, 1H), 4.46 (dd, J = 11.2, 1.4 Hz, 1H), 4.03 (d, J = 11.1 Hz, 1H), 3.33 (d, J = 1.2 Hz, 1H), 3.22 (dd, J = 11.8, 4.1 Hz, 1H), 2.53 (ddd, J = 15.3, 8.0, 3.2 Hz, 1H), 2.46–2.35 (m, 2H), 2.08–1.93 (m, 2H), 1.84 (ddt, J = 12.5, 4.6, 2.3 Hz, 1H), 1.74–1.47 (m, 3H), 1.34 (qd, J = 12.8, 4.1 Hz, 1H), 1.23 (dd, J = 12.9, 2.3 Hz, 1H), 1.18 (s, 3H), 1.11–0.99 (m, 1H), 0.65 (s, 3H); ^{13}C NMR (101 MHz, CD_3OD) δ 171.0, 154.4, 153.0, 151.9, 151.8, 151.7, 148.9, 143.4, 143.3, 126.1, 122.2, 122.2, 116.7, 113.8, 113.6, 108.5, 80.8, 74.6, 72.2, 64.9, 57.7, 56.3, 43.6, 40.2, 38.9, 37.9, 28.9, 26.8, 25.2, 23.4, 15.4; HRMS (ESI): m/z 512.2099 $[M + Na]^+$, calcd for $C_{26}H_{32}FNNaO_7$, 512.2061.

14α-(4′-nitro-phenoxy)-andrographolide (13b)

From **11b** in 82% yield, white solid, mp 163–166 °C. ^{1}H NMR (400 MHz, C_6D_6) δ 8.18–8.13 (m, 2H), 7.25 (m, 1H), 6.91–6.86 (m, 2H), 5.21 (d, J = 10.4 Hz, 1H), 5.00 (d, J = 6.9 Hz, 2H), 4.84–4.79 (m, 2H), 4.18 (d, J = 11.1 Hz, 1H), 3.54–3.46 (m, 1H), 3.32 (d, J = 11.1 Hz, 1H), 2.48 (s, 1H), 2.43–2.35 (m, 1H), 2.13–2.02 (m, 1H), 1.96–1.76 (m, 6H), 1.43–1.14 (m, 6H), 1.25 (s, 3H), 1.23 (s, 3H), 0.66 (s, 3H); ^{13}C NMR (101 MHz, C_6D_6) δ 171.54, 162.43, 147.22, 145.74, 142.21, 134.02, 125.95, 115.01, 109.07, 99.53, 74.96, 72.97, 69.92, 64.28, 52.29, 51.37, 38.36, 38.27, 38.16, 33.92, 30.89, 26.20, 25.85, 25.16, 24.63, 23.45, 16.98; HRMS (ESI): m/z 494.2185 $[M + Na]^+$, calcd for $C_{29}H_{37}NNaO_7$, 494.2155.

14α-(2′-methoxy-4′-nitro-phenoxy)-andrographolide (13g)

From **13g** in 79% yield, white solid, mp 155–159 °C. ^{1}H NMR (400 MHz, CD_3OD) δ 7.93 (dd, J = 8.8, 2.6 Hz, 1H), 7.90 (d, J = 2.6

Hz, 1H), 7.14 (d, J = 8.8 Hz, 1H), 7.05 (dd, J = 9.7, 3.6 Hz, 1H), 5.85 (d, J = 5.7 Hz, 1H), 4.89 (s, 1H), 4.71 (dd, J = 10.9, 5.8 Hz, 1H), 4.65 (s, 1H), 4.44 (dd, J = 10.9, 1.8 Hz, 1H), 4.08 (d, J = 11.1 Hz, 1H), 3.96 (s, 3H), 3.36 (t, J = 5.4 Hz, 2H), 2.56–2.38 (m, 3H), 2.08–1.93 (m, 2H), 1.85 (dd, J = 12.8, 2.5 Hz, 1H), 1.78–1.58 (m, 3H), 1.36 (ddd, J = 25.0, 12.5, 4.0 Hz, 1H), 1.30–1.15 (m, 5H), 0.64 (s, 3H); ^{13}C NMR (101 MHz, CD_3OD) δ 171.45, 153.12, 152.55, 151.94, 148.73, 144.44, 126.18, 118.28, 116.58, 109.47, 108.45, 80.89, 74.76, 72.59, 64.92, 57.18, 56.87, 56.30, 43.66, 39.85, 38.88, 38.16, 28.97, 26.37, 25.18, 23.36, 15.44; HRMS (ESI): m/z: 524.2253 $[M + Na]^+$, calcd for $C_{27}H_{35}NNaO_8$, 524.2260.

General information for assay

Every compound was dissolved in DMSO and diluted with PBS into a stock solution before use. The final concentration of DMSO is 0.1% for all wells. Every experiment was performed in triplicate. Cell culture: 293T cells were maintained in MEM media with 10% fetal bovine serum (FBS), 100 U ml^{-1} penicillin and streptomycin and 1 mM non-essential amino acid under humidified air containing 5% CO_2 at 37 °C.

Transient transfection and FXR luciferase reporter assay[31]

293T cells were plated in 96-well plates at 2.5 × 10^4 per well. After cells attached, 5.0 ng per well pCMV-GAL4-DBD-hFXR-LBD expression vector, 25.0 ng per well pFRLuciferase and 5.0 ng per well Renilla–Luciferase reporter plasmids were transiently transfected into cells using 0.25 μL per well lipofectamine (Invitrogen). After transfection for 18 h, cells were treated with an FXR natural agonist chenodeoxycholic acid (CDCA) at 25 μM in fresh MEM containing 0.5% charcoal-stripped FBS. Then, the synthesized compound was added in gradient concentrations in an antagonist mode. Luciferase activity was measured after an additional 24 h using Dual-Luciferase Reporter Assay System (Promega). The relative antagonistic activity was defined as the ratio of pFRLuciferase activity/Renilla–Luciferase activity and the activity of FXR in the presence of 25.0 μM of CDCA was set as 100%.

Cell viability assay for CC_{50}

293T cells were plated in 96-well plates at 2.5 × 10^4 per well. After being cultured overnight, the cells were exposed to fresh medium containing different concentrations of synthesized compound. After culturing for an additional 24 h, cell viability was determined by 3-(4,5-dimethylthiazol-2-yl)-2,5-diphenyltetrazolium bromide (MTT) assay.

The molecular docking of compounds 10b, 12b, 10g and 12g

The Molecular docking was performed using the Lamarckian Genetic Algorithm as implemented in Autodock 4.2. The crystal structure of the target protein was retrieved from the Protein Data Bank (PDB entry: 3DCT[42]). The docking grids (binding site) were prepared as 60 × 60 × 60 points with a grid spacing of 0.375 Å and centred on the original ligand of the crystal structure. The set of parameters was listed as the following: the size of the population was 150 and the number of energy evaluations was set to 1.0 × 10^7 as the run terminates. For clustering the conformations, the root mean square deviation tolerance was 2.0. Two hundred independent docking runs were carried out for every ligand. ALL other parameters were set to default. Analysis of the results was performed using AutoDockTools and the docked structures were viewed using Discovery Studio 3.5 Client.

Acknowledgements

Authors thank Dr Qian Li for his help of the molecular docking.

Notes and references

1 B. M. Forman, E. Goode, J. Chen, A. E. Oro, D. J. Bradley, T. Perlmann, D. J. Noonan, L. T. Burka, T. McMorris, W. W. Lamph, E. M. Evans and C. Weinberger, *Cell*, 1995, **81**, 687.
2 P. Lefebvre, B. Cariou, F. Lien, F. Kuipers and B. Staels, *Physiol. Rev.*, 2009, **89**, 147.
3 H. Wang, J. Chen, K. Hollister, L. C. Sowers and B. M. Forman, *Mol. Cell*, 1999, **3**, 543.
4 M. Makishima, A. Y. Okamoto, J. J. Repa, H. Tu, R. M. Learned, A. Luk, M. V. Hull, K. D. Lustig, D. J. Mangelsdorf and B. Shan, *Science*, 1999, **284**, 1362.
5 D. J. Parks, S. G. Blanchard, R. K. Bledsoe, G. Chandra, T. G. Consler, S. A. Kliewer, J. B. Stimmel, T. M. Willson, A. M. Zavacki, D. D. Moore and J. M. Lehmann, *Science*, 1999, **284**, 1365.
6 R. Pellicciari, S. Fiorucci, E. Camaioni, C. Clerici, G. Costantino, P. R. Maloney, A. Morelli, D. J. Parks and T. M. Willson, *J. Med. Chem.*, 2002, **45**, 3569.
7 S. M. Soisson, G. Parthasarathy, A. D. Adams, S. Sahoo, A. Sitlani, C. Sparrow, J. Cui and J. W. Becker, *Proc. Natl. Acad. Sci. U. S. A.*, 2008, **105**, 5337.
8 P. R. Maloney, D. J. Parks, C. D. Haffner, A. M. Fivush, G. Chandra, K. D. Plunket, K. L. Creech, L. B. Moore, J. G. Wilson, M. C. Lewis, S. A. Jones and T. M. Willson, *J. Med. Chem.*, 2000, **43**, 2971.
9 M. J. Evans, P. E. Mahaney, L. Borges-Marcucci, K. Lai, S. Wang, J. A. Krueger, S. Gardell, C. Huard, R. Martinez, G. P. Vlasuk and D. C. Harnish, *Am. J. Physiol.: Gastrointest. Liver Physiol.*, 2009, **296**, G543.
10 K. C. Nicolaou, R. M. Evans, A. J. Roecker, R. Hughes, M. Downes and J. A. Pfefferkorn, *Org. Biomol. Chem.*, 2003, **1**, 908.
11 I. Dussault, R. Beard, M. Lin, K. Hollister, J. Chen, J.-H. Xiao, R. Chandraratna and B. M. Forman, *J. Biol. Chem.*, 2003, **278**, 7027.
12 N. L. Urizar, A. B. Liverman, D. T. Dodds, F. V. Silva, P. Ordentlich, Y. Yan, F. J. Gonzalez, R. A. Heyman, D. J. Mangelsdorf and D. D. Moore, *Science*, 2002, **296**, 1703.
13 A. K. Verma, P. Khemaria, J. Gupta, D. P. Singh, B. S. Joshi, R. Roy, A. K. Mishra and R. Pratap, *ARKIVOC*, 2010, **2010**, 1.
14 V. Sepe, G. Bifulco, B. Renga, C. D'Amore, S. Fiorucci and A. Zampella, *J. Med. Chem.*, 2011, **54**, 1314.

15 J. Yu, J. L. Lo, L. Huang, A. Zhao, E. Metzger, A. Adams, P. T. Meinke, S. D. Wright and J. Cui, *J. Biol. Chem.*, 2002, **277**, 31441.
16 S. J. Nam, H. Ko, M. Shin, J. Ham, J. Chin, Y. Kim, H. Kim, K. Shin, H. Choi and H. Kang, *Bioorg. Med. Chem. Lett.*, 2006, **16**, 5398.
17 B. A. Carter, O. A. Taylor, D. R. Prendergast, T. L. Zimmerman, R. Von Furstenberg, D. D. Moore and S. J. Karpen, *Pediatr. Res.*, 2007, **62**, 301.
18 R. Kaimal, X. Song, B. Yan, R. King and R. Deng, *J. Pharmacol. Exp. Ther.*, 2009, **330**, 125.
19 M. Kainuma, M. Makishima, Y. Hashimoto and H. Miyachi, *Bioorg. Med. Chem.*, 2007, **15**, 2587.
20 H. Huang, Y. Yu, Z. Gao, Y. Zhang, C. Li, X. Xu, H. Jin, W. Yan, R. Ma, J. Zhu, X. Shen, H. Jiang, L. Chen and J. Li, *J. Med. Chem.*, 2012, **55**, 7037.
21 J. Y. Chiang, R. Kimmel, C. Weinberger and D. Stroup, *J. Biol. Chem.*, 2000, **275**, 10918.
22 P. A. Edwards, H. R. Kast and A. M. Anisfeld, *J. Lipid Res.*, 2002, **43**, 2.
23 N. Y. Kalaany and D. J. Mangelsdorf, *Annu. Rev. Physiol.*, 2006, **68**, 159.
24 W. Huang, K. Ma, J. Zhang, M. Qatanani, J. Cuvillier, J. Liu, B. Dong, X. Huang and D. Moore, *Science*, 2006, **312**, 233.
25 F. Yang, X. Huang, T. Yi, Y. Yen, D. D. Moore and W. Huang, *Cancer Res.*, 2007, **67**, 863.
26 S. Fiorucci, A. Mencarelli, E. Distrutti, G. Palladino and S. Cipriani, *Curr. Med. Chem.*, 2010, **17**, 139.
27 S. Fiorucci, S. Cipriani, F. Baldelli and A. Mencarelli, *Prog. Lipid Res.*, 2010, **49**, 171.
28 S. Fiorucci, S. Cipriani, A. Mencarelli, F. Baldelli, G. Bifulco and A. Zampella, *Mini-Rev. Med. Chem.*, 2011, **11**, 753.
29 T. A. M. Gulder and B. S. Moore, *Curr. Opin. Microbiol.*, 2009, **12**, 252.
30 K.-H. Lee, *J. Nat. Prod.*, 2010, **73**, 500.
31 W. Liu and C.-W. Wong, *Phytother. Res.*, 2010, **24**, 369.
32 M. K. Gorter, *Recl. Trav. Chim. Pays-Bas Belg.*, 1911, **30**, 151.
33 M. P. Cava, W. R. Chan, L. J. Haynes, L. F. Johnson and B. Weinstein, *Tetrahedron*, 1962, **18**, 397.
34 T. Zhang, *Zhongyaocai*, 2000, **23**, 366.
35 X. Liu, Y. Wang and G. Li, *Zhongyaocai*, 2003, **26**, 135.
36 G.-Z. Liu, H.-W. Xu, K. Sun, J. Wang and H.-M. Liu, *J. Org. Chem.*, 2008, **28**, 201, and references therein.
37 B. Das, C. Chowdhury, D. Kumar, R. Sen, R. Roy, P. Das and M. Chatterjee, *Bioorg. Med. Chem. Lett.*, 2010, **20**, 6947.
38 Z. Wang, P. Yu, G. Zhang, L. Xu, D. Wang, L. Wang, X. Zeng and Y. Wang, *Bioorg. Med. Chem.*, 2010, **18**, 4269.
39 J. C. Lim, T. K. Chan, D. S. Ng, S. R. Sagineedu, J. Stanslas and W. S. Wong, *Clin. Exp. Pharmacol. Physiol.*, 2012, **39**, 300, and references therein.
40 B. Zhou, D. Zhang and X. Wu, *Mini-Rev. Med. Chem.*, 2013, **13**, 298, and references therein.
41 Some of compounds were published in the patent CN103224492 A 20130731 by G.-C. Zhou, C.-W. Wong, Z. Liu, D. Sheng, X. Nie and D. Wang.
42 A. Akwabi-Ameyaw, J. Y. Bass, R. D. Caldwell, J. A. Caravella, L. Chen, K. L. Creech, D. N. Deaton, S. A. Jones, I. Kaldor, Y. Liu, K. P. Madauss, H. B. Marr, R. B. McFadyen, A. B. Miller, F. N. Iii, D. J. Parks, P. K. Spearing, D. Todd, S. P. Williams and G. B. Wisely, *Bioorg. Med. Chem. Lett.*, 2008, **18**, 4339.